THESIS

ESTIMATING INTERSTITIAL DISCHARGE AND VELOCITY IN FLOW IN RIPRAP AND GABION ENGINEERING APPLICATIONS

Submitted by

Anthony Keene

Department of Civil and Environmental Engineering

In partial fulfillment of the requirements

For the Degree of Master of Science

Colorado State University

Fort Collins, Colorado

Fall 2019

Master's Committee:

Advisor: Christopher Thornton
Co-Advisor: Joseph Scalia

John Williams

ABSTRACT

ESTIMATING INTERSTITIAL DISCHARGE AND VELOCITY IN FLOW IN RIPRAP AND GABION ENGINEERING APPLICATIONS

Interstitial flow is a difficult hydraulic process to measure and predict. Interstitial flow does not follow the same laws as seepage flow in small-grain media (i.e. Darcy's Law), because flow regimes in aggregate rock are often transitional or turbulent at a mild slope. Flow paths and local velocities in open cavities of a rock layer are dynamic, and instrumentation is difficult to place in rock for physical measurement. Due to the dynamic and complicated nature of interstitial flow, limited tools are available for engineering flow through aggregate rock.

Flow in aggregate rock is relevant to many hydraulic engineering applications, including riprap and gabions used in designs for drainage, earth retention, and rockfill structures. Riprap and gabion published design guidelines are derived from external flow conditions and often neglect interstitial flow. Discharge in rock directly influences internal forces that can transport loose rock or strain a gabion mattress structure, interstitial velocity also directly influences bed shear stress. However, despite the importance of interstitial velocity and discharge for design, riprap and gabion design guidelines are developed primarily for rock stability. There is a need for interstitial discharge as design criteria; estimating the discharge capacity of aggregate rock can be useful in applications where drainage for a design flow is relevant.

Data from laboratory prototype gabion mattress tests are used in tandem with data collected in a previous study on riprap to develop two simple design equations to predict interstitial velocity and interstitial discharge per unit area of a rock layer. A multivariate

nonlinear regression was performed as a function of the following key parameters in a rock system: rock size for which 50% of rock is finer than, D_{50}, rock size for which 10% of rock is finer than, D_{10}, coefficient of uniformity (D_{60}/D_{10}), acceleration due to gravity, and bed slope. The regressions yield a coefficient of determination of 0.97 for both interstitial velocity and interstitial discharge predictive equations. Equations are suited for use in rock layers with nominal sizes from ¼-in to 5-in on bed slopes up to 0.15 ft/ft.

ACKNOWLEDGEMENTS

First and foremost, I thank my advisor Dr. Christopher Thornton for the opportunity to work with him at the Engineering Research Center and pursue a master's degree at CSU. I have had the privilege to work on this project and many others that have provided me a platform to grow my knowledge and experience in the hydraulic engineering field. His guidance and encouragement have been indispensable in this project and throughout my time here. I would also like to thank my co-advisor Dr. Joseph Scalia for providing his time and expertise to this project. His assistance was fundamental in the completion of this project.

A special thanks to two professors who have been a great influence on me as a hydraulic engineer and a professional in general. I have had the privilege to learn from Dr. Robert Ettema as a student and research assistant. His enthusiasm in hydraulics is unmatched, and my time with him in class and in the lab has been an inspiration. Dr. Donald Chase, a professor and Chair of the Civil Engineering department during my time at my alma mater University of Dayton, played a large role in my decision to pursue a master's degree in hydraulics. His passion and expertise in water resources engineering certainly steered me into my love for hydraulics, and he encouraged me to pursue a master's.

I thank everyone who helped organize, construct, and perform the physical experiments performed for this study. Those I would like to especially thank are Taylor Hogan, Sam Eggleston, and Cody Volt who all put in many hours assisting in the project.

Finally, I thank my family for their continued support throughout my time in graduate school. Mom, Dad, Kelsey, Abbey, Adam, Andrea, thank you!

TABLE OF CONTENTS

LIST OF TABLES

LIST OF FIGURES

LIST OF SYMBOLS

A, B = coefficient in Forchheimer equation describing fluid and material properties

a, b, c, d, e, f, l m, n, o, p = coefficients in multivariate nonlinear power regression

C_u = coefficient of uniformity – D_{60}/D_{10}, dimensionless

D_{10} = 10^{th} percentile rock size

D_{50} = 50^{th} percentile rock size

D_{60} = 60^{th} percentile rock size

i = hydraulic gradient, ft/ft

k = hydraulic conductivity/permeability, ft/s

n_p = porosity, dimensionless

ν = kinematic viscosity, ft^2/s

Q = total discharge, ft^3/s

q = unit discharge, ft^2/s

q' = discharge per ft^2 rock, $ft^3/s/ft^2$

q* = estimated unit discharge per inch of riprap from Abt et al. (1988, 1989) seen in Equation 9, $ft^2/sec/in$

q_m* = measured unit discharge per inch of riprap, $ft^2/s/in$

q_{ik} = estimated discharge per ft^2 rock, from Keene et al. (2019) seen in Equation 14, $ft^3/s/ft^2$

R_e = Reynold's number, dimensionless

S_o = bed slope, ft/ft

V = velocity, ft/s

V_c = calculated velocity based on continuity and porosity in a rock layer, ft/s

V_{i1} = estimated average interstitial velocity from Abt et al. (1988, 1989) used in Equation 7, ft/s

V_{i2} = estimated average interstitial velocity from Abt et al (1988, 1989) used in Equation 8, ft/s

V_{ik} = estimated average interstitial velocity from Keene et al. (2019) used in Equation 13, ft/s

Symbols associated with C.E. Kirkham's Field Equation for estimating velocity in porous media:

a = parameter in energy loss equation

E = Piezometric head

E_x, E_{xx}, E_y, E_{yy}, E_{xy} = symbolic representation of $\partial E/\partial x$, $\partial^2 E/\partial x^2$, $\partial E/\partial y$, $\partial^2 E/\partial y^2$, $\partial^2 E/\partial x \partial y$, respectively

K = parameter in energy loss equation = $1/(a^N)$

K_v = Symbolic representation of $\partial K/\partial v$

N = exponential parameter in energy loss equation

N_v = Symbolic representation of $\partial N/\partial v$

P = $(E_x^2 + E_y^2)$

CHAPTER 1. INTRODUCTION

Studies at Colorado State University (CSU) involving hydraulic engineering applications have revealed a need to examine interstitial flow characteristics in aggregate rock. Interstitial flow characteristics are difficult to define due to the dynamic and variable nature of flow within aggregate rock pores. There is a need for a simple set of equations to provide velocity and discharge values for a wide range of unique sizes and gradations of aggregate rock. Hydraulic performance testing of prototype rock gabion mattresses was performed and has provided data needed to establish simple equations to estimate interstitial velocity and discharge in aggregate rock.

Interstitial flow is a general term describing the movement of fluid flow through the open cavities created by porous media, shown in Figure 1-1, and is found in hydraulic engineering applications where flow is present in granular media such as rock, gravel, and soil.

Figure 1-1 Interstitial flow exiting a rock gabion mattress

Interstitial flow characteristics in any porous media can be difficult to define but are much more so in aggregate rock, as the flow regime is more prone to a turbulent state than in the tight pores of sand and other smaller-grained media (Venkataraman 1998). Flow lines through the voids of rock have varying paths, as shown in Figure 1-2, and also have a varying local velocity that differs from the average velocity. Both direction and speed of a water particle within the voids depend heavily on the characteristics of the rock and the energy grade line of the flow, and both can vary at any point in the rock profile.

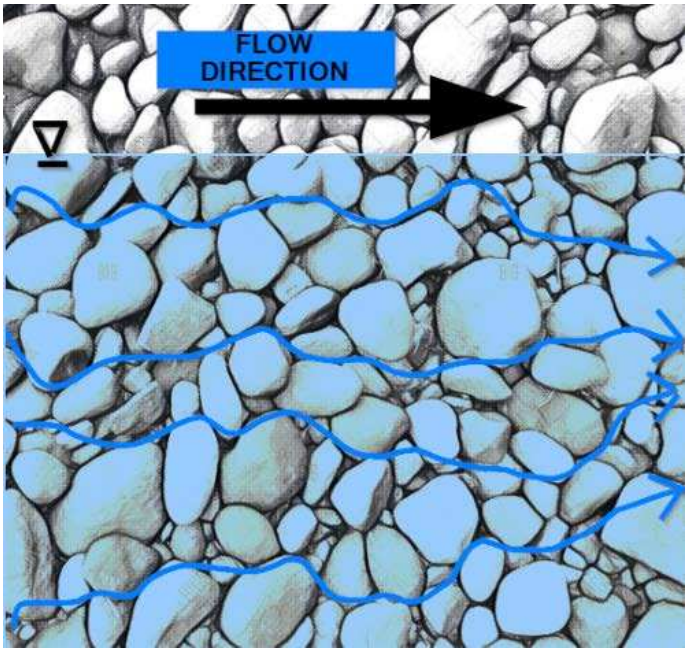

Figure 1-2 Examples of flow paths through aggregate rock

Aggregate rock (herein describing rock diameter sizes from ¼" to 24") is used in a variety of engineering applications such as embankment stabilization, waterway erosion control, and drainage functions. Rock can be applied in many forms including riprap, gabion mattresses, and fill and armor material for structures ranging from rockfill dams and retaining walls to stormwater outlet protection and energy dissipators.

Critical to these applications is an understanding of interstitial flow characteristics of the rock used, including pressure (from depth), velocity, and discharge capacity of the particular rock. High interstitial velocities and depth, which are two main factors that determine the shear stress on the underlaying soil, have the capability to erode the soil bed the rock is meant to protect. Interstitial velocity (also referred to as "through-flow velocity") also has an influence on the internal forces of a rock structure, and therefore can affect the rock stability. Discharge capacity is important because it reveals how quickly a fluid can drain and ultimately exit the area that the rock is protecting or stabilizing. Furthermore, discharge through a rock layer is also important to know if designing for overtopping or flood flows. Discharge through rock can be subtracted out from the original design flow, leaving design engineers with the actual discharge above the rock. For design engineers, knowing interstitial flow characteristics is vital in understanding the effectiveness of a given rock in a particular engineering application.

Existing Riprap and Gabion Design Guidelines

In the past century, numerous studies have been performed to analyze riprap effectiveness. Investigations have focused on riprap performance for revetments, river beds, dam overtopping, and more. From this, publications present empirical equations to find optimum rock size or rock characteristics given parameters such as bed slope, fluid velocity, unit discharge, shear stress, depth, Froude Number, and others – all in a variety of combinations (Julien 2018). Government entities have adopted these studies as well as published design guidelines based on internal studies for engineers to implement in the field. Perhaps the most common riprap design guidelines are the United States Bureau of Reclamation's EM-25 (USBR 1958) and Design Standards No. 13 (USBR 2014), the United States Army Corps of Engineers' EM-1601 (USACE 1994), and the Federal Highway Administration's HEC-11 (FHWA 1989).

Guidelines and the associated internal studies just mentioned, however, focused on stability threshold relationships between the different testing parameters, and not the discharge capabilities of the rock. Stability thresholds are the hydraulic condition(s) (velocity, shear stress, etc.) at which the riprap is either transported or the underlying embankment is corrupted. The purpose of most riprap studies done to supplement published guides has been to observe and document threshold values of the rock at or immediately preceding incipient motion (i.e. transport) or embankment erosion. Current design guidelines, therefore, recommend riprap properties solely based on these failure criteria. Interstitial discharge was not a variable taken into consideration.

Gabion mattresses are similar to riprap and have many of the same applications, but rock is encased in right-angled wire mesh. Design criteria to size riprap to avoid transport can be generally eliminated because of the wire meshes, and the overturning resistance and flexibility of mattresses allow placement on terrain where riprap is not stable. Subsequently, gabions have a more unique domain of applications where riprap may not be suitable, with specific designs to accompany these applications. Applications where gabions may be more suitable than riprap include check dams, embankment stabilization on steep and/or changing slopes, and retaining walls.

Gabion design guidelines are not as prominently published by government agencies as riprap, but are available in engineering journals, experimental reports, and guidelines from gabion manufacturers. Stephenson et al. (1979) provides a series of stability guidelines in *Rockfill in Hydraulic Engineering*, a volume from Developments in Geotechnical Engineering. Design guidelines are included for overturning and sliding stability of single layer and stacked gabions on slopes in water and on horizontal planes in water. Stephenson et al. (1979) also

provides structural arrangements and associated load criteria for use of gabions for retaining walls. Although the permeable nature of rock plays a role in the behavior of forces in gabions, velocity and discharge are not parameters taken into consideration for the stability guidelines offered by Stephenson et al. (1979).

Experimental tests were performed at CSU by Simons et al. (1984) to develop gabion mattress design guidelines. Based on certain design discharges, tests aimed at determining gabion mattress requirements that resisted incipient motion while still effectively preventing underlying erosion. Hydraulic conditions such as shear stress and Manning *n* within the mattress were observed, and relationships were developed to estimate them. Velocity at the interface between the rock and a filter or soil was also studied by Simons et al. (1984), but average interstitial velocity and interstitial discharge were not parameters investigated.

Manufacturers that produce gabions and gabion systems sometimes publish their own design guidelines for the more popular uses of a given product (Global Synthetics 2019). Permeability of gabions is almost always mentioned and is used as a selling point, but there are no guidelines that mention a discharge parameter when sizing rock. Design guidelines, like riprap, are based on failure criteria such as underlying soil erosion and structural failures of the gabion system, and rock sizing is most often based on the gabion dimensions and mesh sizes.

The Rockfill Ford

Rockfill fords are raised rockfill structures built at drainage crossings to protect a road from overtopping flows and debris flows. Rockfill fords are used where a channel crossing requires a high fill for good road alignment, and are typically applied on remote, unpaved roads in steep terrain where streams are prone to high flows or debris flows (U.S. Forest Service 2006). Porous fill allows typical streamflow to pass even if debris is caught, and the rockfill surface

protects the road from overtopping damage in the case of flood flows. An example of a rockfill ford is shown in Figure 1-3.

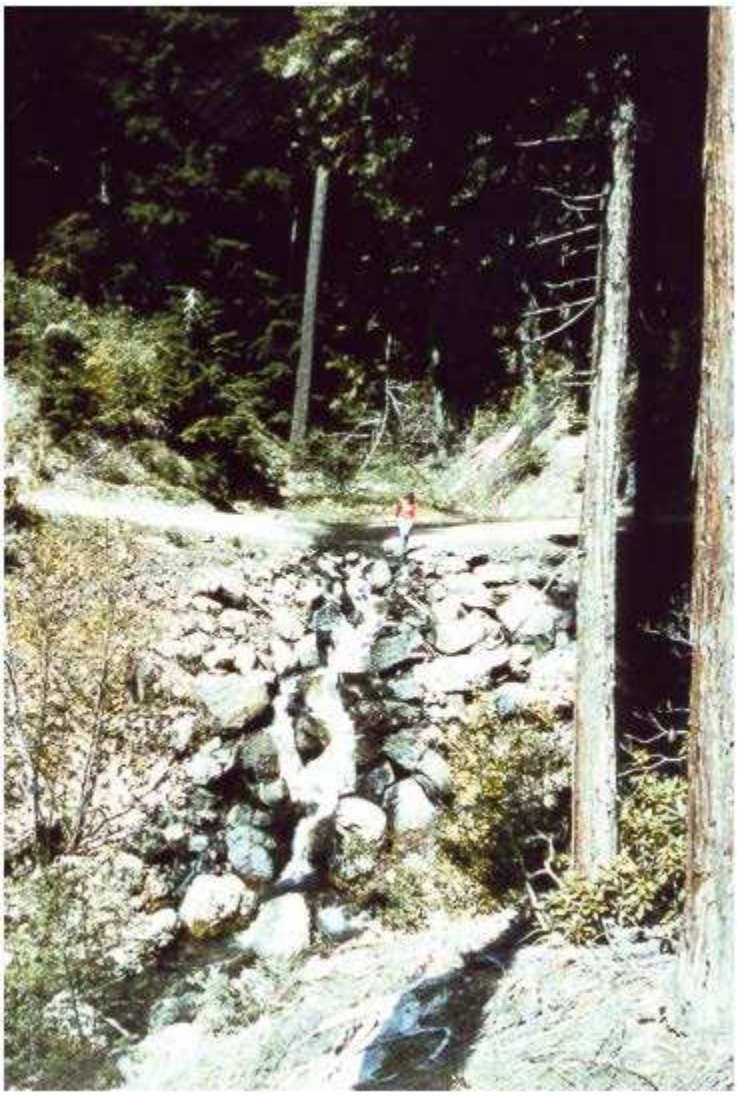

Figure 1-3 Rockfill ford in Oregon (U.S. Dept. of Agriculture 2006)

Unpaved remote roads, such as those used in the logging industry or for the Forest Service, can be faced with erosion and rutting due to poor runoff drainage. Rutting and further road destruction can be especially significant when poor drainage is coupled with traffic from heavy machinery or recreational vehicles. Remote locations, rough terrain, and limited

construction space present difficulties when considering the time, cost, and ultimately practicality of installing an effective drainage system.

A rockfill ford can mitigate these difficulties. First, materials used can be gathered from nearby locations, reducing cost and potentially construction time. Native rock can be transported from a nearby location and used as the fill for the ford. Also, construction of a rockfill ford is relatively straightforward. Excavation and fill may be required, but steep terrain streams are not typically wide, making the construction area small. Once the drainage crossing is set, rock material can be dumped and moved easily to finish the crossing, avoiding complications of installing culverts, bridges, or other structures.

Design of a rockfill ford is typically not quantitative. Rock size is determined by the largest available rock, and the slope of the rockfill is normally adjusted to the average stream slope (U.S. Forest Service 2006). In view of this, rockfill fords can be applied in a variety of configurations under an engineer's discretion. Designs have been known to use culverts in tandem with rockfill fords when cost and construction constraints allow. Alternatively, the reverse is also used, where rockfill fords are constructed to compliment an existing pipe that may not be adequate or has already been clogged by debris flow. Figure 1-4 shows a profile sketch of this application. In the case where a road is not prone to overtopping, rockfill can be placed underneath the road with no protection on top, making a rock-only "culvert" as shown in Figure 1-5.

Considering the current state of practice for rockfill fords, there is a need for a quantitative design basis. An equation for estimating discharge through rock based on rock size, gradation, and rockfill layer area can be directly applied to rockfill ford designs.

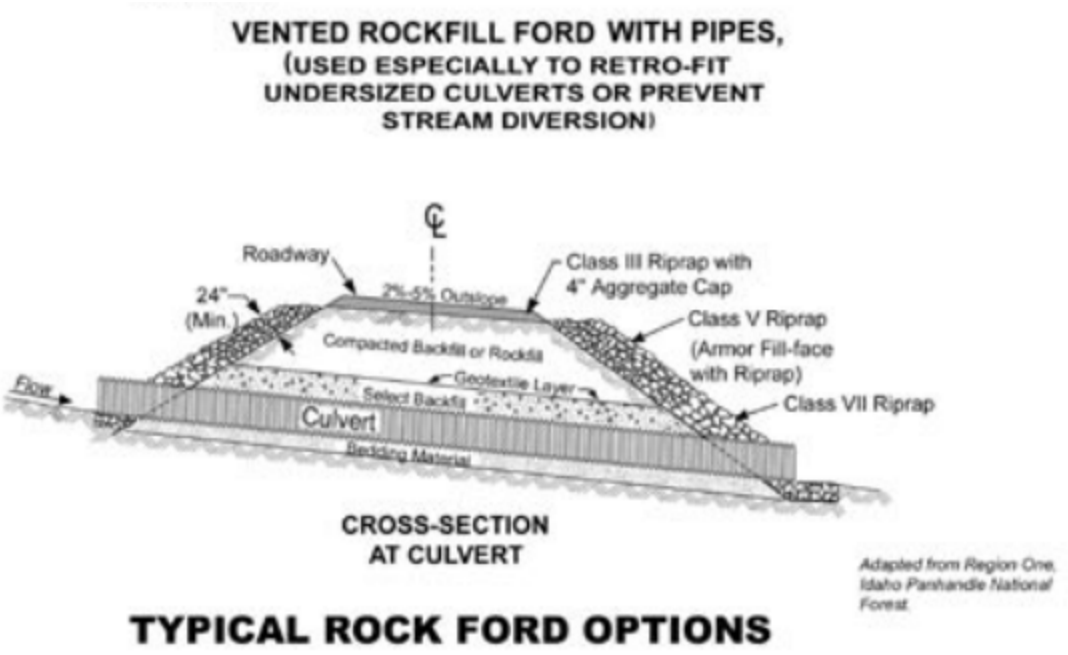

Figure 1-4 Sketch of design example of rockfill ford complimenting an existing culvert (U.S. Forest Service 2006)

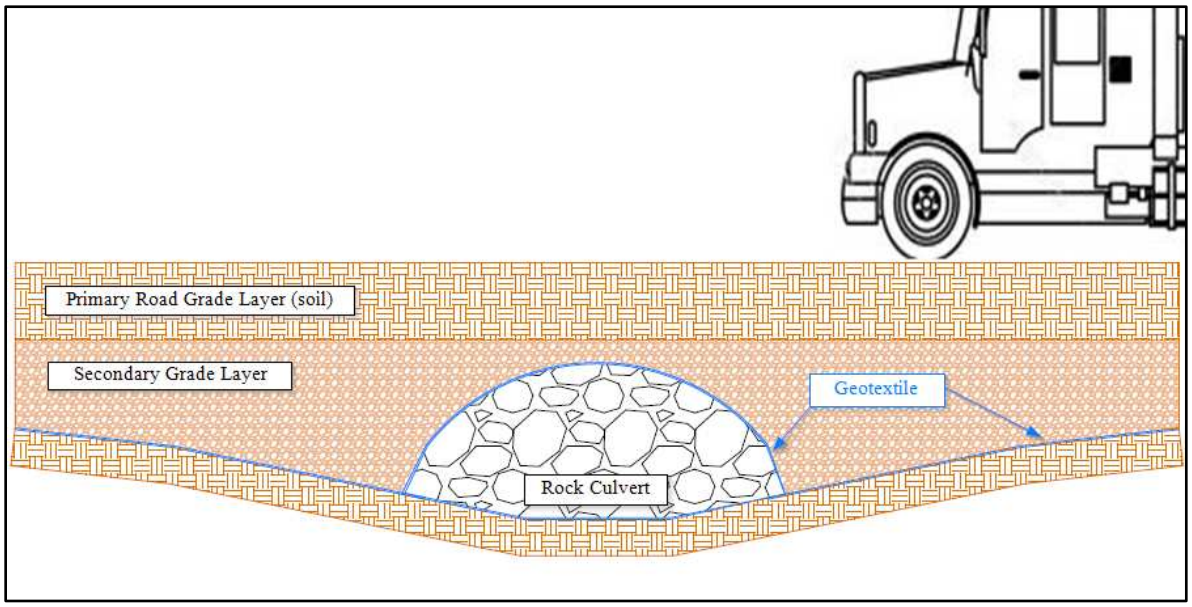

Figure 1-5 Example cross section sketch of rockfill culvert

Important Characteristics of Aggregate Rock in Engineering Design

Similar to the rockfill ford, many other engineering applications depend on drainage of water from and through aggregate rock. In erosion control applications, rock can double as an effective drainage layer, as water must need to be conveyed away from the areas that require protection. For example, on river banks and riverbeds, not inhibiting the cross-sectional area of the flow is important to not reduce conveyance, as reducing the cross-sectional area will raise the depth of water upstream. The pores in the rock provide flow paths and maintain some conveyance to avoid unwanted water level increases. On road embankments and culvert outlets, rainfall runoff should not be allowed to pool and weaken the surrounding soil. Material stabilizing the protected earth needs to have effective drainage capabilities. When in use on a check structure or retaining wall, aggregate rock ensures quick dissipation of hydrostatic pressure that can build up behind the structure. Aggregate rock is also not limited to dual erosion control and drainage applications and can also be used solely for drainage purposes. Rock can be found in bedding for underground pipe installations, railroad ballasts, French drains and other drainage curtains (Judge 2013). Rock is an accepted material for use in these applications because rock does not hold water and can still be used as a sturdy fill.

Objectives

The objectives of this study are listed as follows.

1. Document the rock characteristics that most influence interstitial discharge and velocity
2. Develop an empirical equation to estimate average interstitial velocity in aggregate rock that is a function of characteristics easily attainable to a design engineer
3. Develop an empirical equation to estimate discharge in aggregate rock that is a function of characteristics easily attainable to a design engineer

General Study Outline

Previous studies conducted at CSU by Abt et al. (1987, 1988) also aimed at better understanding interstitial flow characteristics in aggregate rock, but for the purpose of riprap design. Abt et al. (1987, 1988) presented empirical interstitial velocity and discharge equations in these studies. This paper presents data gathered from flume experiments for the current study and from previous flume studies by Abt et al. (1987, 1988) on interstitial flow in aggregate rock. The current and previous studies both measured flow rate and velocity according to bed slope in combination with varying rock characteristics. Flume experiments for this study used a variety of rock sizes and gradations in 2-foot and 6-foot wide flumes with adjustable slopes, and measurements included flow rate and water surface elevations.

An analysis was performed to first validate equations developed by Abt et al. (1987, 1988) with the data from the current study, followed by an analysis of both data sets to understand the influence of certain experimental parameters. Then, analyses to adjust and redevelop previous empirical equations was made to provide improved equations that would be of more practical use in design. Two improved equations presented in this study predict interstitial velocity and unit discharge as a function of parameters that could be easily found or calculated by a design engineer. Candidate rock characteristics considered for inclusion in redeveloped empirical equations include median rock size D_{50}, rock size D_{10}, and coefficient of uniformity in tandem with bed slope.

CHAPTER 2. BACKGROUND

A summary of current knowledge related to interstitial flow in aggregate rock and related topics is provided. Predictive relationships for interstitial flow have been derived or developed empirically, but a simple and effective design equation is absent in the current state of the practice to predict velocity and discharge in aggregate rock.

Darcy's Law

Darcy's Law, shown in Equation 1, is an experimentally validated relationship that describes flow in a porous medium, viz. specific discharge is linearly proportional to the hydraulic gradient (Chin 2013).

$$V = Ki \tag{1}$$

where:

V = bulk (macroscopic) velocity (Length/Time)

i = hydraulic gradient (Length/Length)

K = hydraulic conductivity/permeability (Length/Time)

Darcy's Law applies to laminar and some transitional flow regimes. As the Reynold's number, defined in Equation 2, increases in the flow through pores in a given media, viscous forces become less dominant and the relationship between specific discharge and hydraulic gradient (Darcy's Law) becomes nonlinear (Chin 2013). The Reynold's Number (R_e) for flow through porous media is a function of specific discharge (also referred to as bulk velocity), V, in feet per second, the grain size at which ten percent of the material is finer than, D_{10}, and kinematic viscosity of the fluid, v (Chin 2013).

$$R_e = \frac{VD_{10}}{\nu} \quad (2)$$

where:

R_e = Reynold's number (dimensionless)

V = specific discharge (ft/s)

D_{10} = grain size at which 10% of the material is finer than by mass (ft)

ν = kinematic viscosity (ft^2/sec)

Studies conducted by Ahmed and Sunada (1969) and Bear (1972) indicate that deviations from Darcy's Law occur when $R_e > 1$ and strong deviations when $R_e > 10$. Reynold's Numbers for flow in aggregate rock sizes greater than ¼-in are orders of magnitude greater than 10 (Chin 2013). Therefore, the K found in the design guidelines derived from Darcy's Law are not appropriate to compare to discharge in aggregate rock.

The Forchheimer Equation

The Forchheimer Equation, shown in Equation 3, is a formula that also describes the relationship between i and V in flow in porous media (Chin 2013). Unlike Darcy's Law, the Forchheimer Equation relates these variables for nonlinear flows in transitional and turbulent regimes (Venkataraman et al. 1998).

$$i = AV + BV^2 \quad (3)$$

where:

A, B = constants, depending on the porous media and fluid properties, respectively

Although the Forchheimer Equation can apply to the flows in this study and roughly predict velocity in some aggregate rocks, Equation 3 is difficult to use for design engineers. First, coefficients A and B have not been studied sufficiently to be provided values for given fluid and rock properties. Some studies suggest that these constants need to be found experimentally on case-by-case bases (Venkataraman et al. 1998). Other studies have employed different methods to determine *A* and *B*, such as by dimensional analysis as described by Ward (1964) and using the Navier-Stokes equation to develop equations for *A* and *B* as described in Ahmed and Sunada (1969). Both methods are too difficult and time consuming to use the Forchheimer equation for design applications.

Kirkham's Field Equation for Velocity in Porous Media

Kirkham (1967) developed a general field equation to predict velocity in a porous medium applicable to all flow regimes in large particle size porous medias for which Darcy's Law does not apply. Kirkham's Field Equation, shown in Equation 4, was developed around a partly graphical, partly mathematical correlation between energy gradient and velocity and may be applied when an energy gradient-velocity relationship is available for the porous medium.

$$\left(E_{xx} + E_{yy}\right) + \left(\frac{E_x^2 E_{xx} + 2E_x E_y E_{xy} + E_y^2 E_{yy}}{P}\right) * \left(\frac{2K(N-1) + V(2K_V + KN_V \log_e P)}{2K - V(2K_V + KN_V \log_e P)}\right) = 0 \quad (4)$$

where:

E = Piezometric head

E_x, E_{xx}, E_y, E_{yy}, E_{xy} = symbolic representation of $\partial E/\partial x$, $\partial^2 E/\partial x^2$, $\partial E/\partial y$, $\partial^2 E/\partial y^2$, $\partial^2 E/\partial x \partial y$, respectively

$P = (E_x^2 + E_y^2)$

K = parameter in energy loss equation = $1/(a^N)$

a = parameter in energy loss equation

N = exponential parameter in energy loss equation

K_v = Symbolic representation of $\partial K/\partial v$

N_v = Symbolic representation of $\partial N/\partial v$

Easy application for a design engineer are lacking from the Kirkham Field Equation. Velocity and flow rate are not explicitly shown and are concealed in the piezometric head variables, and the necessary input parameters are not readily available. Furthermore, rock characteristics are absent from this equation, which are essential independent variables in the engineering design using aggregate rock.

Colorado State University Studies for Riprap Design Criteria

Abt et al. (1987, 1988) performed a two-phase study at CSU on the topic of riprap failure and riprap design criteria. Abt et al. (1987, 1988) used a series of laboratory flume experiments to replicate embankment overtopping conditions to gather hydraulic data for analysis. Analyses aimed to determine riprap stability thresholds as well as understand interstitial flow behavior in different rock characteristics like size, shape, and gradation. Experiments varied bed slope and flow rate. Among the many objectives of the Abt et al. (1987, 1988) studies, a unique set of the experimental program included tests solely to gather data for interstitial flow. Objectives for these tests were to develop equations to predict interstitial velocities and flow rates for given rock characteristics. Objectives of Abt et al. (1987, 1988) – as well as how a portion of the interstitial data was gathered – matches the objectives and data gathering processes for this study.

Throughout the two phases of the Abt et al. (1987, 1988) interstitial flow sub-study, more than twenty unique tests were conducted in two different flumes, where measurements were

taken on flow through varying rock and filter blanket configurations. Flow meters were used to measure discharges, but to measure velocity, a tracer solution injection system was used inside the rock layer. Injections were released inside the rock at the upstream end and tracer-sensitive probes were used to detect tracer at the downstream end. Table 2-1 summarizes the interstitial sub-study data reported by Abt et al. (1987, 1988). A more in-depth evaluation of the experimental processes, flume drawings, and results is presented in Abt et al. (1987, 1988).

Abt et al. (1987, 1988) provided a validation to the velocities measured by comparing the data to a calculated velocity, V_c. Calculated flow velocity, shown in Equation 5, uses the continuity equation, shown in Equation 6, while factoring in porosity and cross-sectional area, A. Equation 6 includes the assumption that porosity, n_p, multiplied by the total rock layer area is a representation of the true effective flow area.

$$V_c = \frac{Q}{An_p} \tag{5}$$

$$Q = VA \tag{6}$$

Where:

Q = discharge (ft^3/sec)

A = cross sectional area of flow (ft^2)

V_c = calculated velocity (ft/s)

n_p = porosity (dimensionless)

Table 2-1 Interstitial flow experimental data from Abt et al. (1987,1988)

Test ID	**Rock Width** Ft	**Rock Height** Ft	D_{50} Inches	D_{10} Inches	C_u -	n_p -	S_o ft/ft	Q cfs	V_m ft/s	V_c ft/s
6 I	8.0	0.25	1.0	0.60	1.75	0.44	0.010	0.11	0.10	0.13
7 I	8.0	0.25	1.0	0.60	1.75	0.44	0.020	0.11	0.13	0.13
9 I	8.0	0.25	1.0	0.60	1.75	0.44	0.100	0.21	0.24	0.24
4 I	8.0	0.50	2.2	1.10	2.09	0.45	0.010	0.23	0.15	0.13
3 I	8.0	0.50	2.2	1.10	2.09	0.45	0.020	0.33	0.23	0.18
10 I	8.0	0.50	2.2	1.10	2.09	0.45	0.100	0.56	0.36	0.31
11 I	8.0	0.50	2.2	1.10	2.09	0.45	0.100	0.56	0.37	0.31
26 II	12.0	0.25	2.0	1.03	2.14	0.45	0.100	1.11	0.46	0.82
28 II	12.0	0.33	2.0	1.03	2.14	0.45	0.100	1.16	0.47	0.65
28 II	12.0	0.33	2.0	1.03	2.14	0.45	0.100	0.91	0.50	0.55
30 II	12.0	0.50	2.0	1.03	2.14	0.45	0.100	1.84	0.63	0.68
30 II	12.0	0.50	2.0	1.03	2.14	0.45	0.100	1.79	0.54	0.63
33 II	12.0	0.67	2.0	1.03	2.14	0.45	0.100	2.05	0.50	0.47
33 II	12.0	0.67	2.0	1.03	2.14	0.45	0.100	2.11	0.59	0.46
35 II	12.0	0.50	4.0	2.05	2.12	0.36	0.100	0.97	0.40	0.50
35 II	12.0	0.50	4.0	2.05	2.12	0.36	0.100	0.94	0.55	0.46
37 II	12.0	1.00	4.0	2.05	2.12	0.36	0.100	3.05	0.58	0.73
37 II	12.0	1.00	4.0	2.05	2.12	0.36	0.100	4.20	0.73	0.83
43 II	12.0	1.00	4.0	2.00	2.30	0.45	0.100	3.33	0.84	0.64
47 II	12.0	1.00	4.0	1.20	4.00	0.39	0.100	2.46	0.35	0.53
39 II	12.0	0.50	4.0	2.00	2.30	0.45	0.100	2.40	0.49	0.82
39 II	12.0	0.50	4.0	2.00	2.30	0.45	0.100	2.52	0.62	0.67
41 II	12.0	0.67	4.0	2.00	2.30	0.45	0.100	2.52	0.72	0.56
41 II	12.0	0.67	4.0	2.00	2.30	0.45	0.100	2.37	0.66	0.57
3 I - 2	12.0	1.00	4.1	2.00	2.15	0.44	0.200	4.34	0.72	0.82
4 I - 2	12.0	1.00	4.1	2.00	2.15	0.44	0.200	4.25	0.97	0.80
50 II	12.0	1.00	4.0	2.38	1.72	0.46	0.100	4.64	0.91	0.86
50 II	12.0	1.00	4.0	2.38	1.72	0.46	0.100	5.58	0.66	0.99
8 I	12.0	1.00	5.1	3.45	1.62	0.46	0.200	5.70	1.04	1.03
9 I - 2	12.0	1.00	5.1	3.45	1.62	0.46	0.200	5.96	0.86	1.08
14 I	12.0	1.00	6.2	3.80	1.69	0.46	0.200	6.22	1.51	1.13

Figure 2-1 illustrates measured velocity against the calculated velocity from the Abt et al. (1987, 1988) study. A linear trendline was fitted to the data and is shown against the black line, which would represent a perfect one-to-one correlation. Abt concluded that there was a good correlation between the two velocities and that the measured velocities were acceptable.

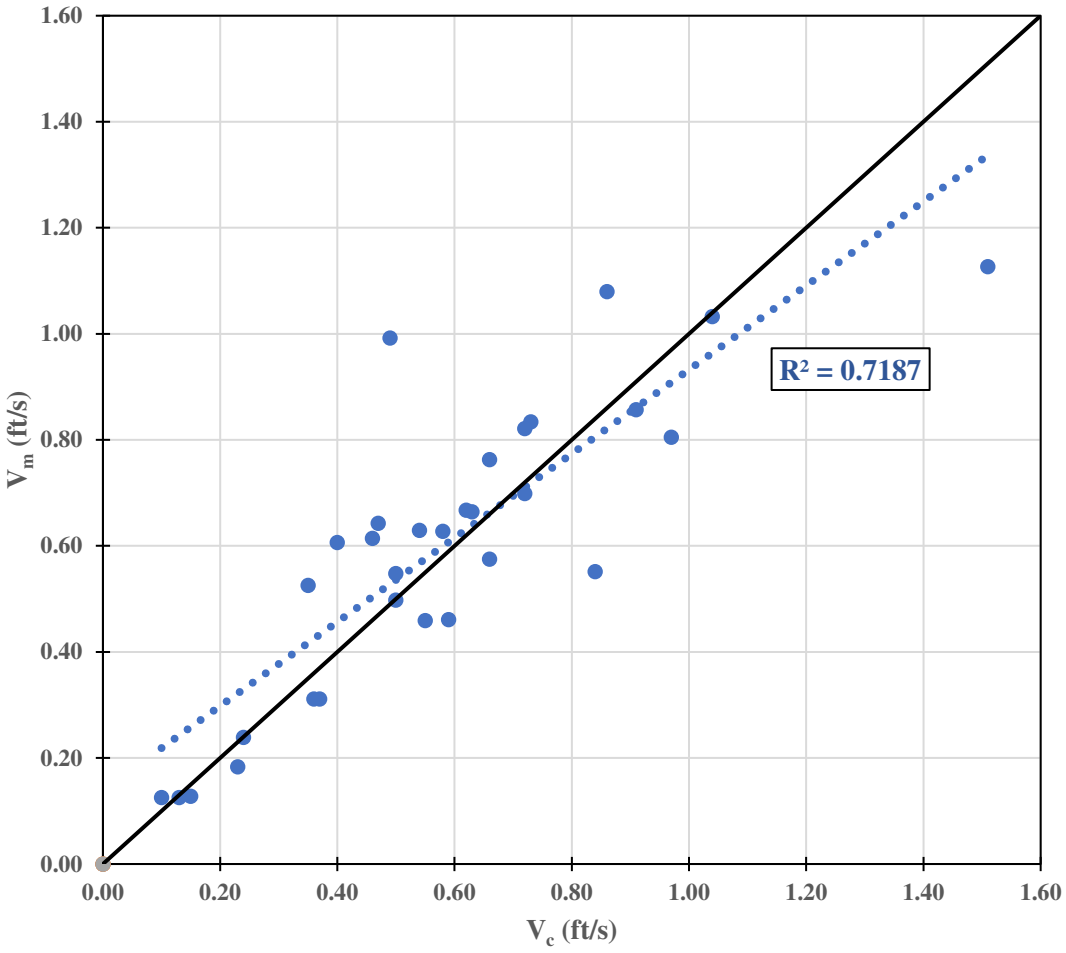

Figure 2-1 Abt et al. (1987, 1988) measured interstitial velocity versus velocity calculated by continuity

With the interstitial velocity data, Abt et al. (1987, 1988) then performed a multivariate power regression and developed two different empirical equations to predict interstitial velocities as a function of a combination of the following: stone size D_{50}, stone size D_{10}, porosity, n_p, bed slope, S_o, coefficient of uniformity, C_u (D_{60}/D_{10}), and acceleration due to gravity, g.

V_{i1} represents the velocity calculated by Equation 7 with D_{10} in inches, S_o, and g. V_{i2} is the velocity found using Equation 8 with the same units for acceleration due to gravity and bed slope as in V_{i1}, but D_{50} is in feet.

$$V_{i1} = 0.232\sqrt{gD_{10}S_o} \tag{7}$$

$$V_{i2} = 19.29\left(C_u^{-0.074}S_o^{0.46}n_p^{4.14}\right)^{1.064}\sqrt{gD_{50}} \tag{8}$$

where:

V_{i1} = velocity by Abt first equation – from Equation 7 (ft/s)

V_{i2} = velocity by Abt second equation – from Equation 8 (ft/s)

g = acceleration due to gravity, 32.2 ft/s^2

S_o = bed slope (ft/ft)

C_u = coefficient of uniformity (dimensionless), D_{60}/D_{10}

Figure 2-2 illustrates the measured velocity data versus the velocity values found using Equation 7 and 8. This plot shows how well the equations predict interstitial velocity against the actual measured values. A linear best fit is also plotted for both data sets. Equations 7 and 8 predict the velocity of the data set from which the data sets were derived with good correlation, with R^2 of 0.80 and 0.73 for V_{i1} and V_{i2}, respectively. For comparison, a line of perfect agreement is plotted alongside the best fit lines for V_{i1} and V_{i2}.

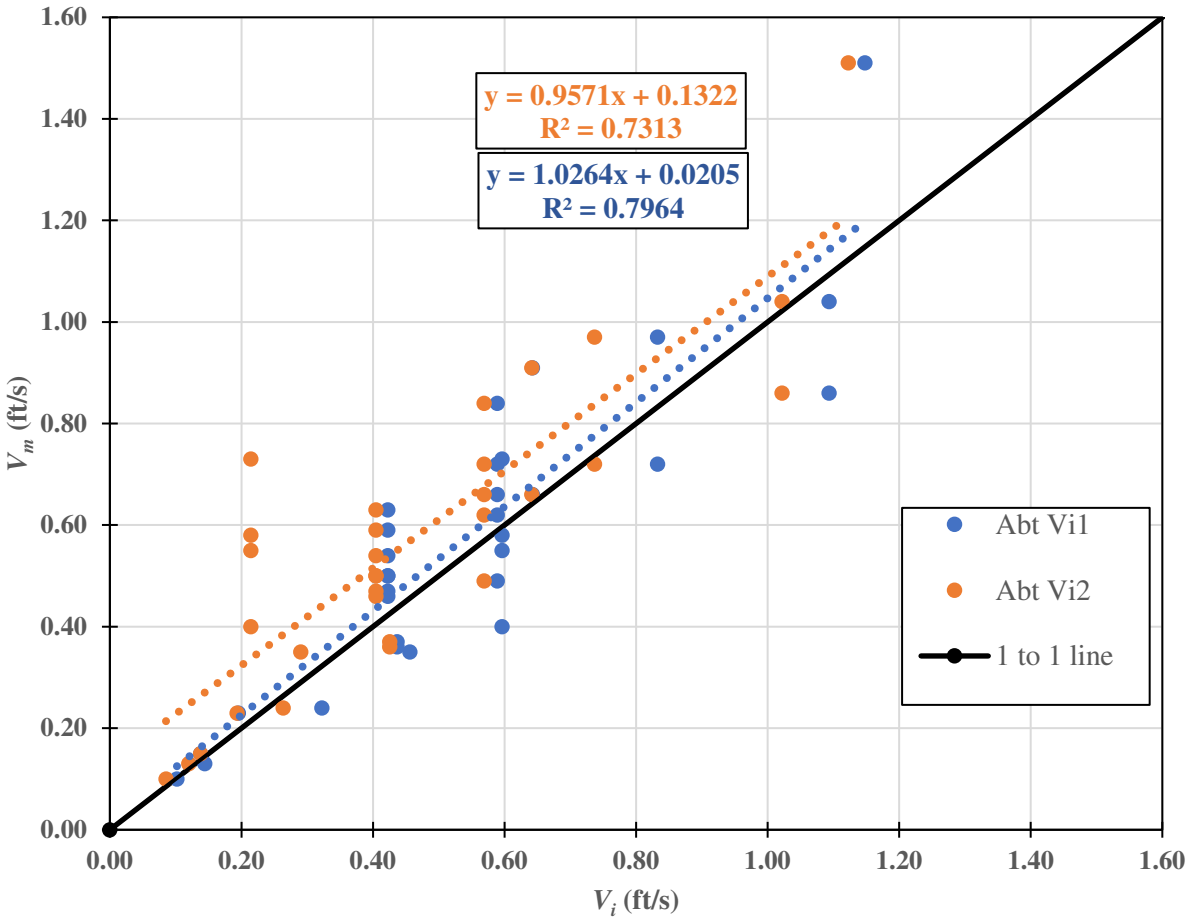

Figure 2-2 Measured velocity data versus estimated velocity by equations V_{i1} and V_{i2}

Abt et al. (1987, 1988) also developed an equation to predict interstitial discharge, shown below in Equation 9, based on the same variables as presented in Equation 8.

$$q^* = 0.079\left(C_u^{-0.94} S_o^{0.46} n_p^{1.07}\right)^{0.999} \sqrt{gD_{50}} \quad (9)$$

where:

q^* = unit discharge per inch of riprap thickness (ft^2/sec/in)

Equation 9 provides an estimation of unit discharge per inch of riprap thickness, with units of square feet per second per inch. Measured discharge values from Abt et al. (1987, 1988)

tests, symbolized as q_m*, versus estimated q* values from Equation 9 are plotted in Figure 2-3. Based on the results plotted in Figure 2-3, Equation 9 estimates unit discharge per inch of rock well. A best-fit line of the data yields an R^2 value of 0.69, and the best fit line has a slope of 1.02

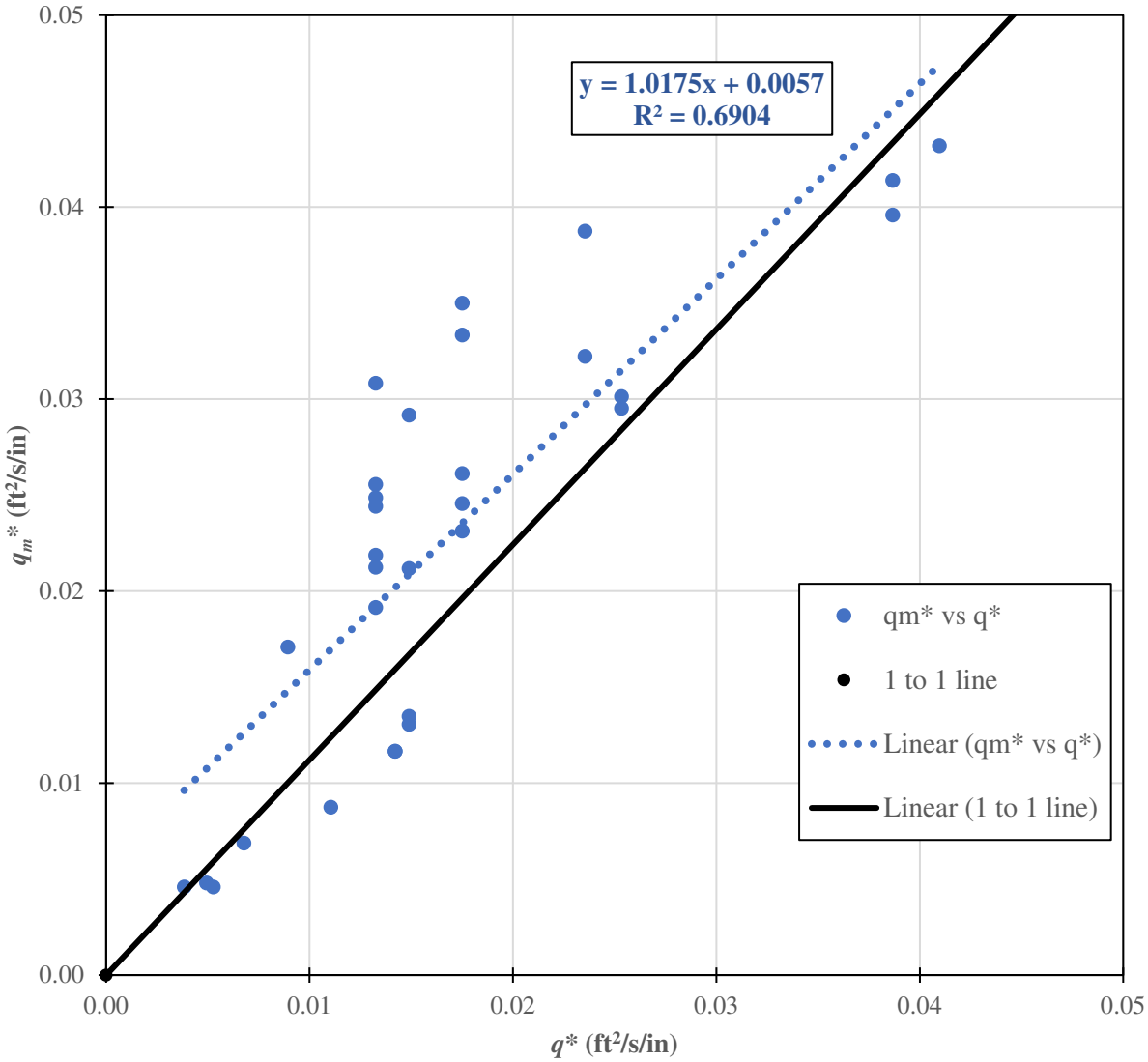

Figure 2-3 Comparison of measured and predicted unit discharge per inch of riprap thickness

. Equation 7- 9 have limitations. First, both Equation 7 and Equation 8 underpredict velocity, and Equation 9 underpredicts unit discharge. Second, the range of data to which the equations are derived is from tests at small flow velocities (0-1.5 ft/s) and unit discharge (0-0.05 ft^2/s/inch). Third, the vertical stratification seen in all three equations shows where multiple tests with the same input parameters outputted diverse values. Equations 7- 9 may not hold up in other rock with a more diverse set of properties. New data is needed to validate these equations.

CHAPTER 3. EXPERIMENTAL PROGRAM

To develop an equation for use by design engineers, additional data are required to add to the data set already compiled by Abt et al. (1987, 1988). Supplemental data needs to expand on the parameters already used by Abt et al. (1987, 1988) in order to encompass rock characteristics suited for applications other than riprap. Additionally, supplemental data needs to assist in developing conclusions on the influence of parameters on interstitial velocity and discharge as well as strengthen existing conclusions observed by Abt et al. (1987, 1988). Rock with sizes and gradations suitable for typical use in gabion mattress systems were selected to be a part of this experimental program. Additionally, one experimental rock set tested in this study was coarse gravel which was not tested by Abt et al. (1987, 1988). A description of the rock tested is detailed in a later section of this chapter. Table 3-1 presents the experimental program matrix.

Experimental Facilities

Flume experiments were used to collect data needed for this study. Flumes are used to create controlled flow environments that can replicate field conditions without the difficulty of field data collection. Experiments took place in the flume facilities at CSU's Hydraulics Laboratory at the Engineering Research Center. Prototype gabion mattresses were used to test different rock parameters in these flumes and were filled to full through-flow. The entire vertical and horizontal profile of the mattresses was conveying flow and no surface water above the mattress was delivered. Three flumes A, B, and C were used for this study.

Table 3-1 Currents study's experimental program test matrix

Test ID	D_{50}	D_{10}	C_u	n_p	S_o
Flume-No.	Inches	Inches	-	-	ft/ft
A-1	3.0	2.25	1.5	0.47	0.025
A-2	3.0	2.25	1.5	0.47	0.035
A-3	3.0	2.25	1.5	0.47	0.045
A-4	3.0	2.25	1.5	0.47	0.050
A-5	3.0	2.25	1.5	0.47	0.080
A-6	4.0	3.00	1.5	0.49	0.016
A-7	4.0	3.00	1.5	0.49	0.025
A-8	4.0	3.00	1.5	0.49	0.025
A-9	4.0	3.00	1.5	0.49	0.035
A-10	4.0	3.00	1.5	0.49	0.035
A-11	4.0	3.00	1.5	0.49	0.045
A-12	4.0	3.00	1.5	0.49	0.045
A-13	4.0	3.00	1.5	0.49	0.050
A-14	4.0	3.00	1.5	0.49	0.050
A-15	4.0	3.00	1.5	0.49	0.080
A-16	4.0	3.00	1.5	0.49	0.080
A-17	4.0	4.00	1.0	0.47	0.025
A-18	4.0	4.00	1.0	0.47	0.025
A-19	4.0	4.00	1.0	0.47	0.035
A-20	4.0	4.00	1.0	0.47	0.035
A-21	4.0	4.00	1.0	0.47	0.045
A-22	4.0	4.00	1.0	0.47	0.050
A-23	4.0	4.00	1.0	0.47	0.080
B-1	4.0	4.00	1.0	0.47	0.150
C-1	0.5	0.25	2.0	0.45	0.060
C-2	0.5	0.25	2.0	0.45	0.120
C-3	0.5	0.25	2.0	0.45	0.138

Flumes A and B Facility and Experimental Description

Flumes A and B used the same dimensions and prototype gabion configurations. Both had a 2-foot width between side walls. Tests were run on Flume A at slopes 1.6, 2.5, 3.5, 4.5, 5.0 and 8.0% with a 30-foot length of rock and Flume B at a slope of 15% with a 26-foot length of rock. Figure 3-1 and Figure 3-2 display a Flume A profile image and profile schematic, respectively. Figure 3-3 and Figure 3-4 display a Flume B profile image and profile schematic, respectively. Tests on Flume A and B used rockfill encased in gabion wire mattresses that measured 1-foot in height and 2-feet in width as shown in Figure 3-5. Tests in Flume A and B also had a geotextile filter fabric lining the bed.

Flume A uses a circulating sump system with a variable speed pump to control the flow rate. Flow enters through a head box and exits back to the sump after 60 feet of flume length along a steel bed and plexiglass sidewalls. The test section was approximately 30 feet long situated in the middle of the flume, where a test bed was installed underneath the rock to replicate bed roughness that could be seen in the field. Concrete masonry blocks made up the bed for the 10.5 feet of the upstream and downstream ends of the test section. A soil embankment 12 feet long and 6 inches thick was constructed between the blocks and compacted according to ASTM D6460. To complete the bed in the test section, a 200 mg/m^2 geotextile filter fabric was glued and anchored down with angle irons on the flume sidewalls. The fabric stretched the entire length of the test section. Rock was placed in gabion wire mattresses and set approximately 10 feet downstream of the headbox to avoid entrance turbulence upon reaching the rock. The rock section was filled three 3-meter-long gabion mattresses totaling approximately 30 feet in length, and free flowing exit conditions were maintained in all tests to avoid tailwater effects that would influence the interstitial flow characteristics in the mattresses.

Figure 3-1 Flume A profile image

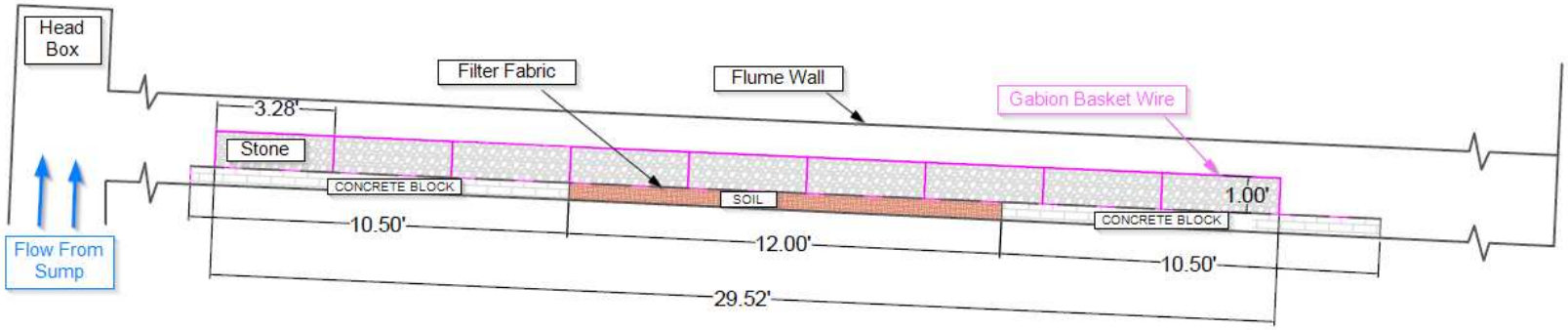

Figure 3-2. Flume A profile schematic

Figure 3-3 Flume B profile image

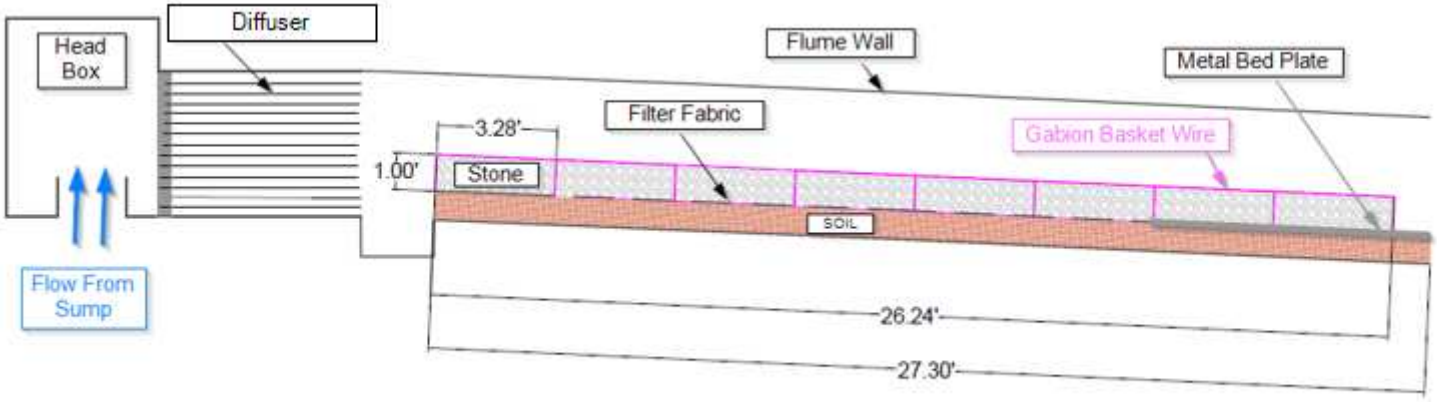

Figure 3-4 Flume B profile schematic

Figure 3-5. Prototype gabion mattresses used in flume tests A and B

Flume B also uses a circulating sump system, but the pump has a fixed speed. A gate valve regulates flow just before entering the pipe that delivers water to the flume headbox, and a butterfly valve regulates flow at a bypass in the system upstream from the gate valve. In the headbox, flow is straightened through a series of PVC pipes and discharged into the flume channel. A 6-foot-long metal plate lined the bed outside the test section to avoid exit effects and head cutting of the embankment. The flume has waterproofed wood and composite wood for

sidewalls. Apart from the length of flume (30 feet) and length of rock (26 feet), the flume bed configuration is the same as Flume A.

Data measured in the Flume A and B tests included discharge and water surface elevations. Discharge was measured in the pipes delivering flow to the flume using a George Fischer Signet 2550 Magmeter for Flume A and a Rosemount pressure transmitter and annubar for Flume B. Both flumes have a data acquisition cart, shown in Figure 3-6, that could reach any point of the test sections. A point gage accurate to 0.01 feet was attached to the carts and recorded water surface elevations.

Figure 3-6 Data acquisition cart and point gage

Flume C Experimental Description

Flume C is 6-foot wide between side walls and 30 feet long. Flume C tests were run at 6.0, 12.0, and 13.8% slope and using a geomat configuration with a 1-foot thick layer of rock between two geomats, all above a 1-foot thick compacted soil embankment. A profile image and profile schematic of the flume is shown in Figure 3-7 Figure 3-8.

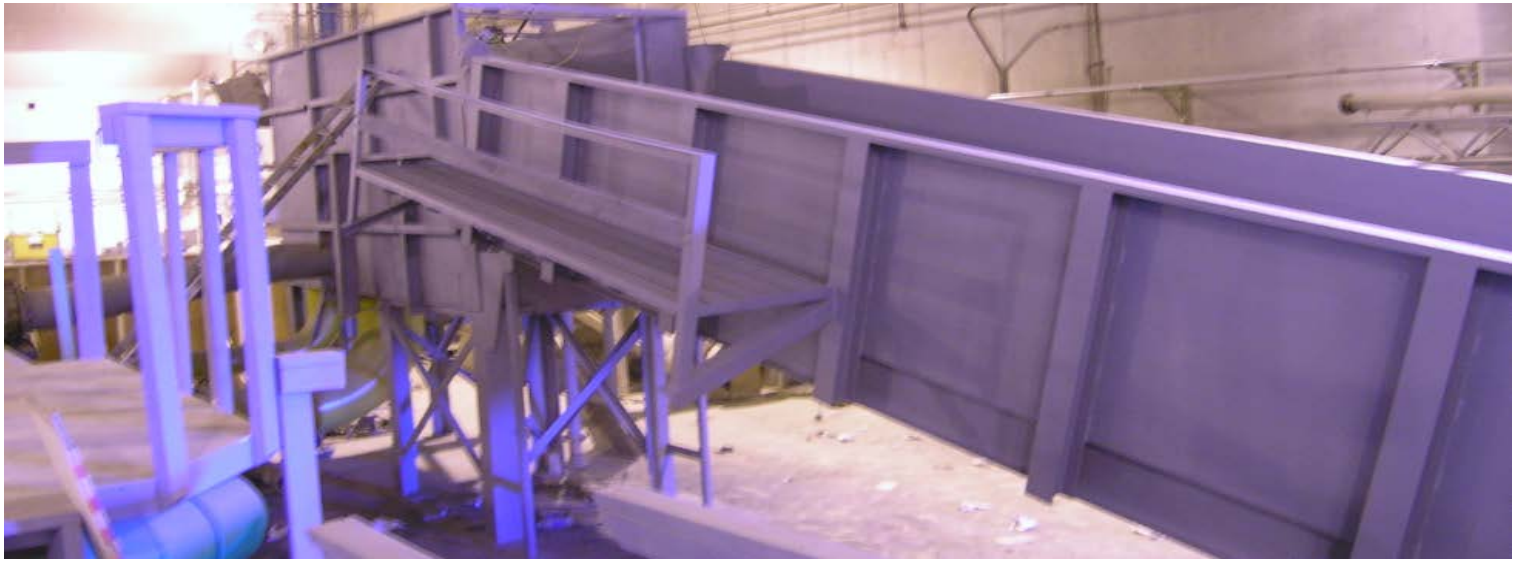

Figure 3-7 Flume C profile image

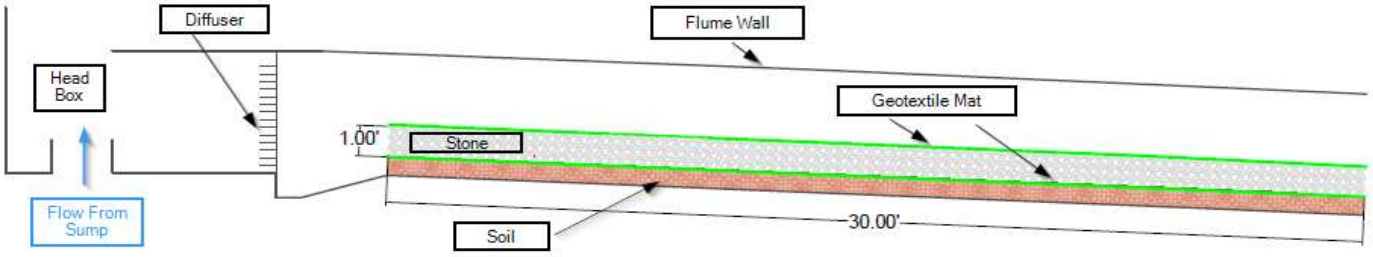

Figure 3-8 Flume C profile schematic

Flume C has a circulating sump system and a pump with a fixed speed. A butterfly valve controls the discharge into the flume, where water fills the headbox and is transported through a series of diffusers. Discharge was measured in the pipes delivering flow to the flume using an Endress+Hauser Promag 53 Magmeter. Immediately after the diffusers, an approach ramp guides the flow in to the beginning of the 30 feet of flume length. The geomats above and below the rock are tightly woven – flow through the geomats was assumed to be insignificant. A soil embankment 30 feet long was constructed underneath the geomat system and compacted according to ASTM D6460. The test section was the full 30 feet length of flume, and free flowing exit conditions were maintained to avoid tailwater effects that would influence the interstitial flow characteristics in the mattresses.

Rock Configurations Tested, Sieve Processes, and Gradation Curves

Four unique rock configurations were tested in this study. Different combinations of size and gradations made up one rock "configuration." Minimum and maximum rock sizes in these tests ranged from 0.25-in to 5.0-in with varying C_u. A higher C_u value describes a more well-graded rock. C_u around 1.0 is poorly graded, meaning the rock sizes are mostly uniform. Table 3-2 contains the characteristics of each rock configuration tested.

Table 3-2 Rock configurations tested in the experimental program

Flume	**D_{50}**	**D_{10}**	**C_u**	**n_p**
	inches	inches	-	-
A	4.00	3.00	1.5	0.372 - 0.488
A	3.00	2.25	1.5	0.395 - 0.465
A & B	4.00	4.00	1.0	0.395 - 0.470
C	0.50	0.25	2.0	0.450

All rock was provided from a local supplier and was a mix of rounded and angular. Rock for tests in Flume A and B were sorted and sieved on site according to the desired gradation. Three, four, and five inch sieves were used and shown in Figure 3-9 and Figure 3-10. The resulting granular size distributions are presented in Figure 3-11. To meet the gradations required, remaining rock was hand-sorted after using the sieves. Rock used in the Flume C tests were sorted and sieved from the supplier before arriving at CSU. Gradation curves for each rock configuration are displayed in Figure 3-11 and sieve data are summarized in Table 3-3.

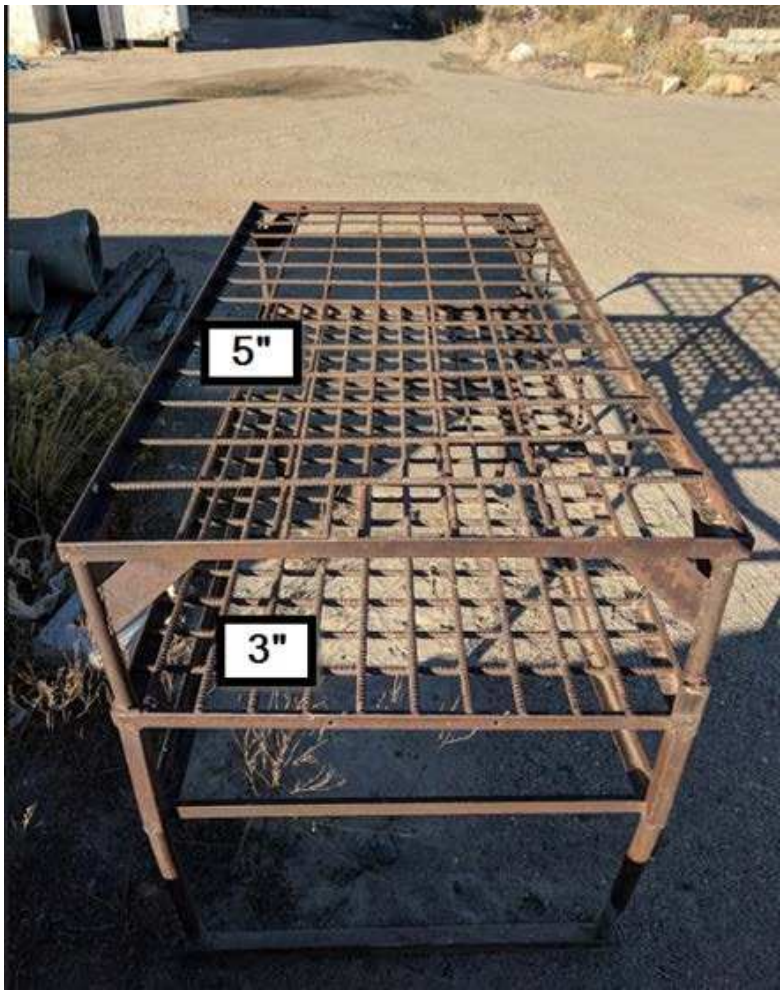

Figure 3-9 Three and five-inch sieve used to grade the rock used in Flume A and Flume B tests

Figure 3-10 Four-inch sieve used to grade the rock used in Flume A and Flume B tests

Table 3-3 Sieve curve data

D_{50}=4.0-in, C_u=1.5		D_{50}=3.0-in, C_u=1.5	
% finer	in	% finer	in
0	2.50	0	2.10
10	3.00	10	2.25
50	4.00	50	3.00
60	4.50	60	3.50
100	5.00	100	4.00
D_{50}=4.0-in, C_u=1.0		**D_{50}=0.5-in, C_u=2.0**	
% finer	in	% finer	in
0	3.50	0	0.25
10	4.00	10	0.25
50	4.00	50	0.50
60	4.00	60	0.50
100	4.25	100	1.00

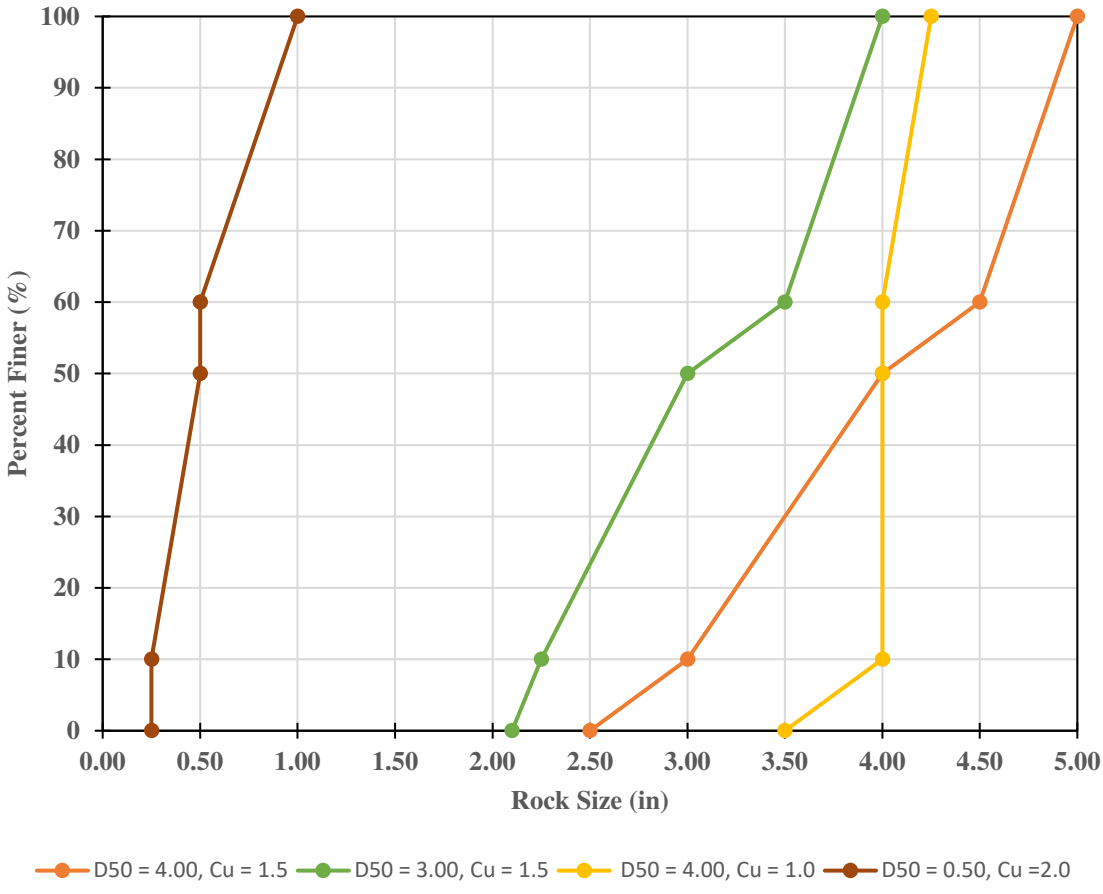

Figure 3-11 Sieve curves for rock tested in the experimental program

Porosity was measured on site for all rock, including rock used in Flume C testing. A closed container with a known volume was used for measuring porosity. After weighing the container and then the container filled with rock, the container was filled with water and the weight difference of water and specific weight of water was used to calculate the volume of voids in the rock. Multiple measurements were taken for each rock configuration and a range of porosities was recorded. For this study, the maximum porosity was used in analysis, which is discussed in Chapter 4.

Experimental Procedure

All tests were performed with the same procedure. After the flume and mattress configuration were constructed and the slope of the test set, flow was discharged into the headbox. Flow was gradually increased to inundate the rock mattress layer. Depending on the flume, the pump speed or valve openings were adjusted until the water surface was at or just above the rock layer. Discharge was then recorded and subsequently held constant until the remaining data measurement was completed. Water surface elevations were taken. Location and number of water surface measurements depended on the test. Table 3-4 lists the tests performed and associated measured and calculated values from the experimental program. In all, twenty-seven unique tests were performed using four different rock configurations.

Table 3-4 Current study experimental program data table

Test ID	D_{50}	D_{10}	C_u	n_p	S_o	i	Q	V_c
Flume-No.	in	in	-	-	ft/ft	ft/ft	cfs	ft/s
A-1	3.0	2.25	1.5	0.47	0.025	0.030	0.72	0.77
A-2	3.0	2.25	1.5	0.47	0.035	0.041	0.85	0.90
A-3	3.0	2.25	1.5	0.47	0.045	0.049	0.92	0.98
A-4	3.0	2.25	1.5	0.47	0.050	0.056	0.94	1.00
A-5	3.0	2.25	1.5	0.47	0.080	0.087	0.98	1.04
A-6	4.0	3.00	1.5	0.49	0.016	0.020	0.77	0.79
A-7	4.0	3.00	1.5	0.49	0.025	0.029	0.77	0.79
A-8	4.0	3.00	1.5	0.49	0.025	0.027	0.83	0.85
A-9	4.0	3.00	1.5	0.49	0.035	0.038	0.87	0.89
A-10	4.0	3.00	1.5	0.49	0.035	0.036	0.92	0.94
A-11	4.0	3.00	1.5	0.49	0.045	0.050	0.93	0.95
A-12	4.0	3.00	1.5	0.49	0.045	0.048	0.97	0.99
A-13	4.0	3.00	1.5	0.49	0.050	0.052	1.02	1.04
A-14	4.0	3.00	1.5	0.49	0.050	0.053	1.03	1.05
A-15	4.0	3.00	1.5	0.49	0.080	0.082	1.19	1.21
A-16	4.0	3.00	1.5	0.49	0.080	0.081	1.16	1.18
A-17	4.0	4.00	1.0	0.47	0.025	0.030	0.64	0.68
A-18	4.0	4.00	1.0	0.47	0.025	0.028	0.78	0.83
A-19	4.0	4.00	1.0	0.47	0.035	0.040	0.74	0.79
A-20	4.0	4.00	1.0	0.47	0.035	0.037	0.89	0.95
A-21	4.0	4.00	1.0	0.47	0.045	0.050	0.79	0.84
A-22	4.0	4.00	1.0	0.47	0.050	0.055	0.83	0.88
A-23	4.0	4.00	1.0	0.47	0.080	0.083	0.97	1.03
B-1	4.0	4.00	1.0	0.47	0.150	0.151	1.49	1.59
C-1	0.5	0.25	2.0	0.45	0.060	-	0.30	0.11
C-2	0.5	0.25	2.0	0.45	0.120	-	0.60	0.22
C-3	0.5	0.25	2.0	0.45	0.138	-	0.53	0.20

CHAPTER 4. DATA INTERPRETATION

An interpretation of the current and past study results is presented. First, data generated from this study are input into the equations developed by Abt et al. (1987, 1988) and plotted to analyze the validity of these equations with the new data. Next, an analysis of the discharge and velocity results of the current study is presented, where influence of test parameters on both dependent variables (velocity and discharge) are observed. Identical analyses are then presented with using the indoor flume data from Abt et al. (1987, 1988) together with the current study data. Conclusions on parameters that most influence discharge and velocity are presented.

Abt Equation Analysis with Current Study Data

Calculated velocity and measured discharge from the current study were input into the equations developed by Abt (described in Chapter 2) and repeated in Equation 7, Equation 8, and Equation 9 for ease of comparison.

$$V_{i1} = 0.232\sqrt{gD_{10}S_o} \tag{7}$$

$$V_{i2} = 19.29\left(C_u^{-0.074}S_o^{0.46}n_p^{4.14}\right)^{1.064}\sqrt{gD_{50}} \tag{8}$$

$$q^* = 0.079\left(C_u^{-0.94}S_o^{0.46}n_p^{1.07}\right)^{0.999}\sqrt{gD_{50}} \tag{9}$$

Outputs comparing calculated parameters from Equations 7-9 were compared to V_c and measured unit discharge per inch of rock in Figure 4-1 and Figure 4-2, respectively. Figure 4-2 shows a converted discharge in units of cubic feet per second per square foot of rock to simplify comparison. Discharge in cubic feet per second per square foot of rock is designated herein as *q'*.

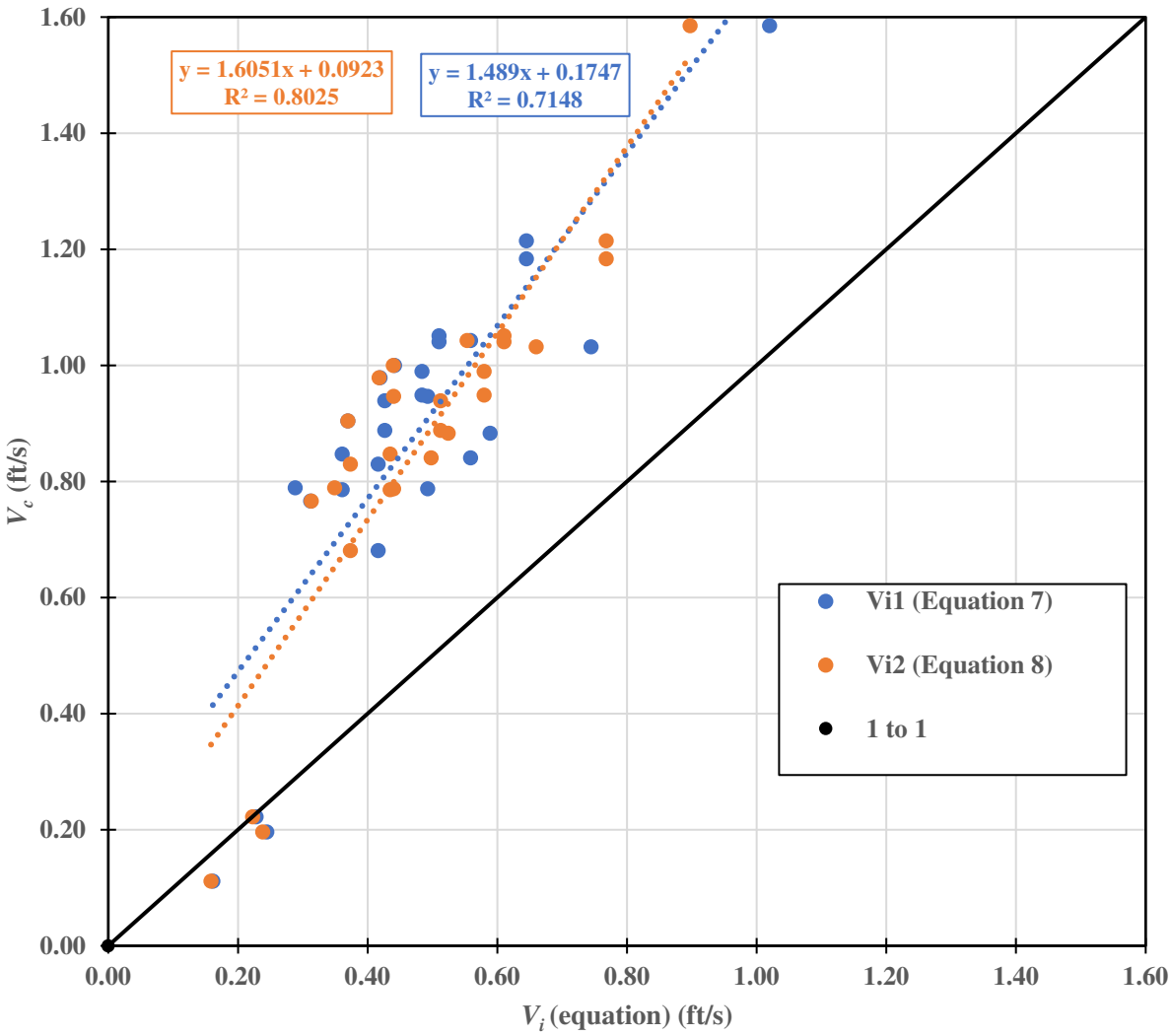

Figure 4-1 Calculated test velocity vs. velocity estimated from current study data input in to Equations 7 and 8

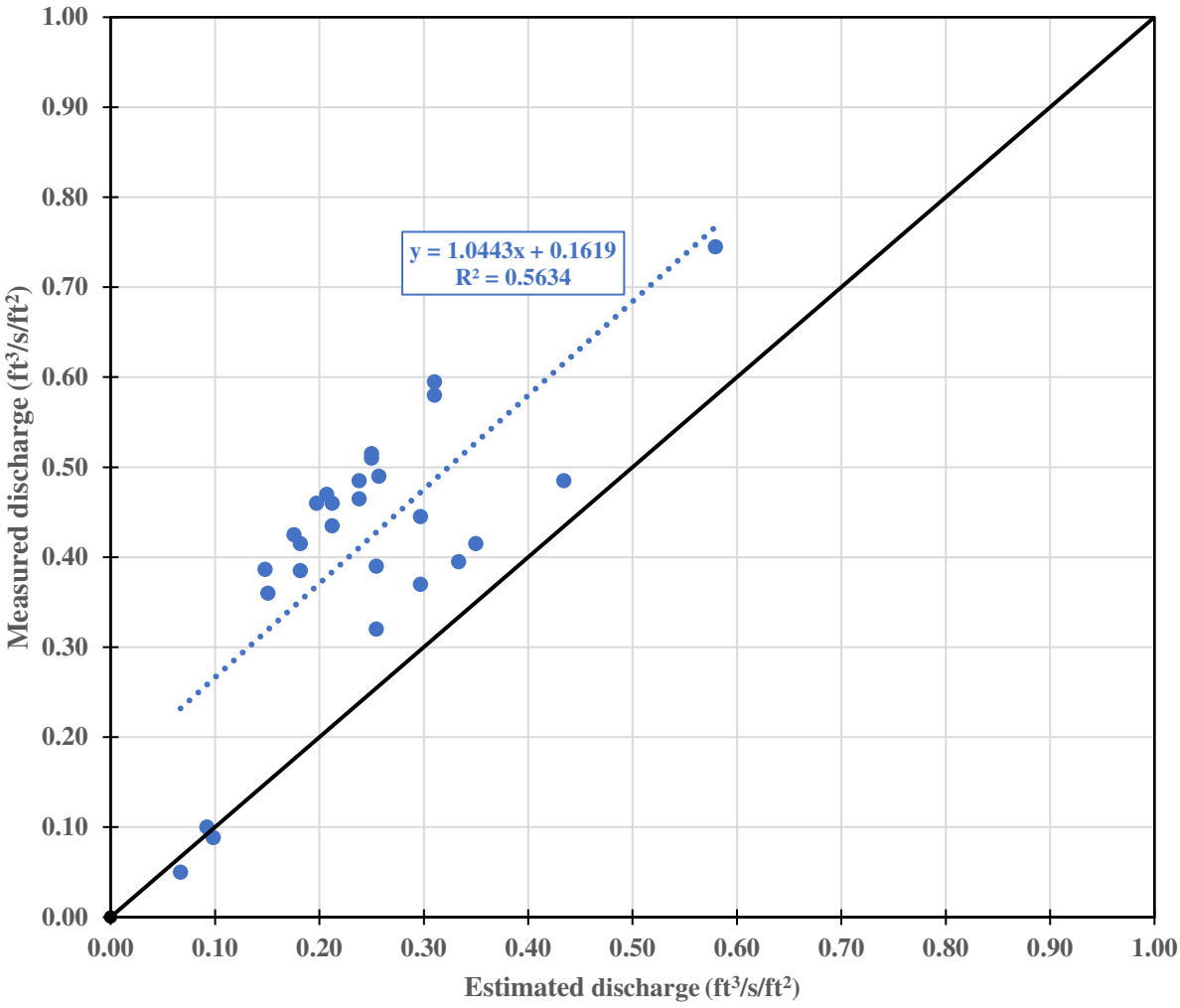

Figure 4-2 Measured discharge vs estimated using data from the current study input into Equation 9

Figure 4-1 illustrates that Equation 7 does not estimate average interstitial velocity well when evaluated with data form the current study. Equation 7 generally underestimates values and the best fit line has a slope of 1.49, indicating a poor correlation between measured and estimated velocity. Figure 4-1 displays that Equation 8 also does not estimate interstitial velocity well when employed with data form the current study and also generally underestimates velocity. Although the line of best fit for discharge values in Figure 4-2 has a slope of 1.02, the weak R^2 of 0.56 illustrates Equation 9 does not produce a good correlation with the current study data.

Based on the comparisons presented in Figures 4-1 and 4-2, updated equations to estimate interstitial velocity and discharge are needed. Influence of test parameters included in the equations also needs to be revisited, as a new equation should include all significant parameters while only using those that can be readily known by a design engineer. The following sections present the discharge and interstitial velocity data from the current study to establish hydraulically relevant parameters.

Discharge Results

Discharge measurements, as seen in Table 3-4 in Chapter 3, are plotted in Figure 4-3 through 4-6 and a qualitative analysis is presented on the significance of relevant test parameters. Data are color separated by rock size.

Data presented in Figures 4-3 to 4-6 illustrate that there is a positive linear relationship between discharge through the rock in terms of either bed slope or hydraulic gradient. Bed slope and hydraulic gradient values for a given test result are insufficiently different to differentiate these parameters. The shape of the data changes minimally comparing Figure 4-3 to 4-4 and Figure 4-5 to 4-6 when the bed slope and hydraulic gradient are interchanged on the x-axis.

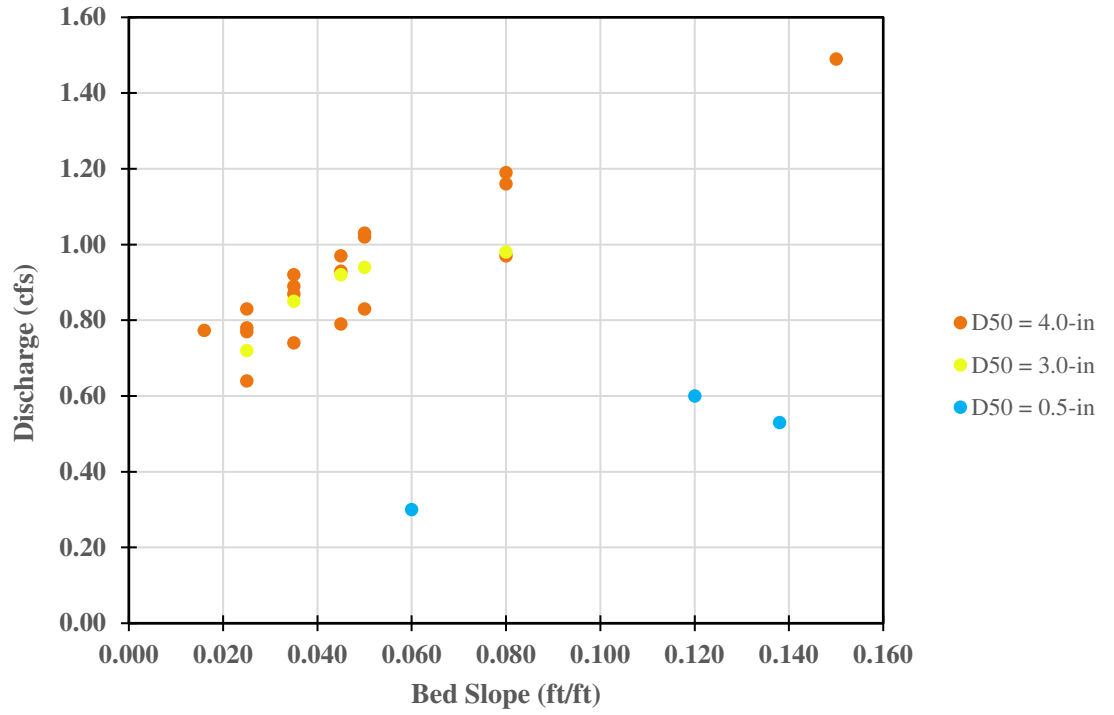

Figure 4-3 Discharge versus bed slope for different D_{50} values, current study data only

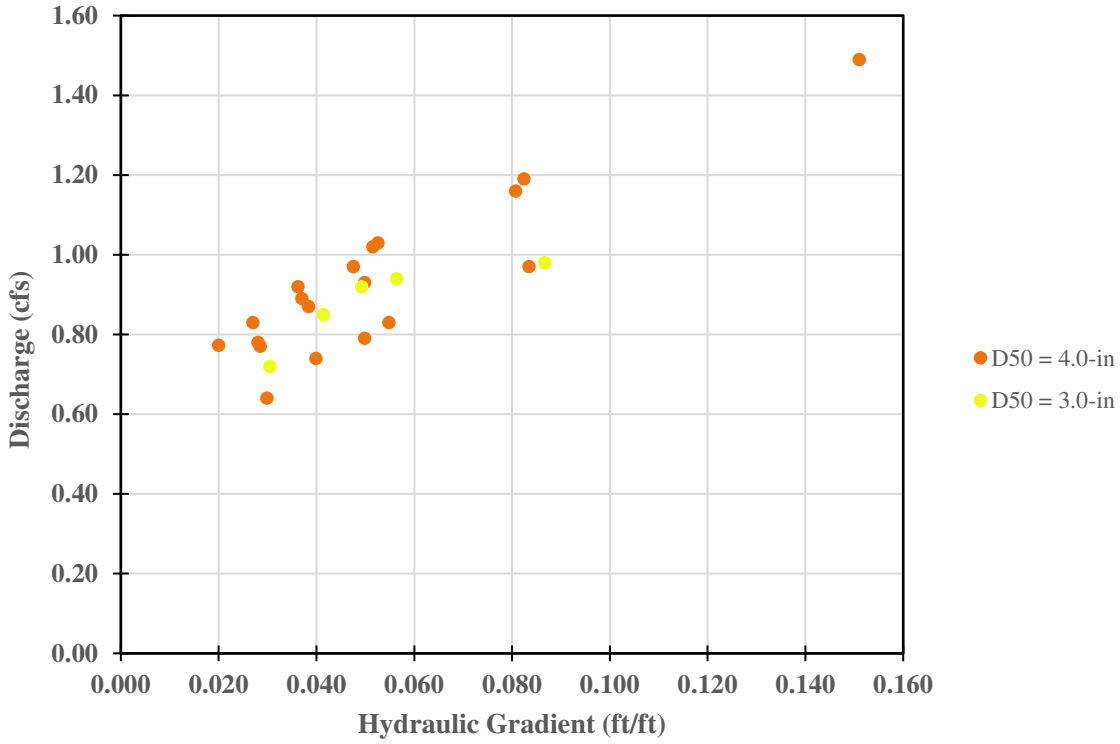

Figure 4-4 Discharge versus hydraulic gradient for different D_{50} values, current study data only

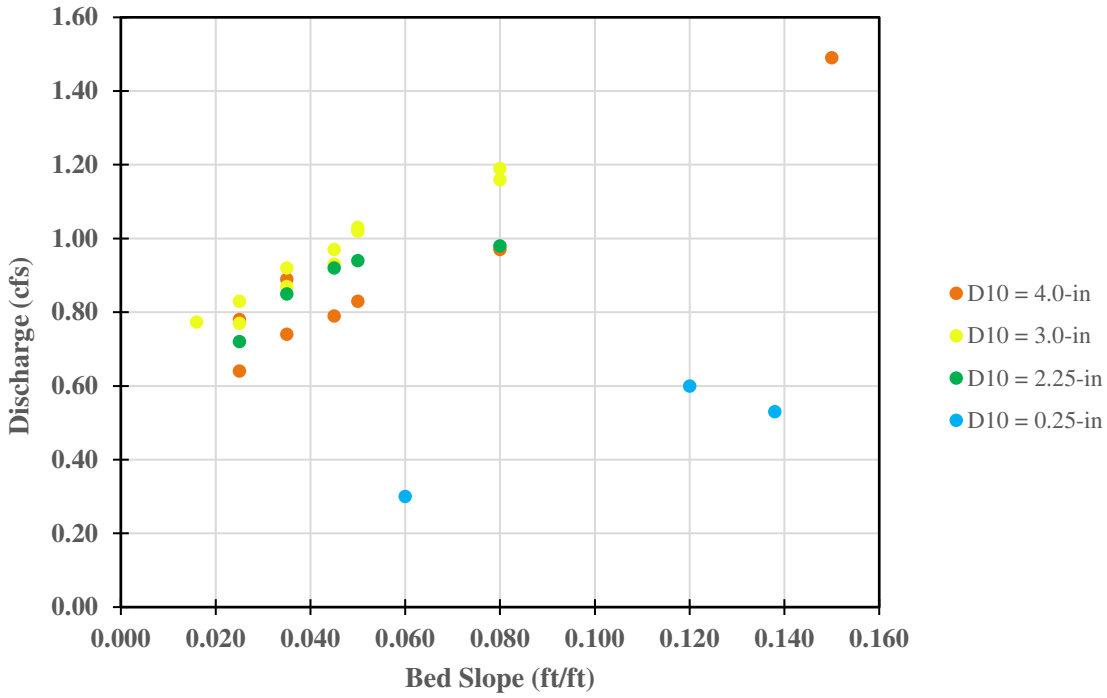

Figure 4-5 Discharge versus bed slope for different D_{10} values, current study data only

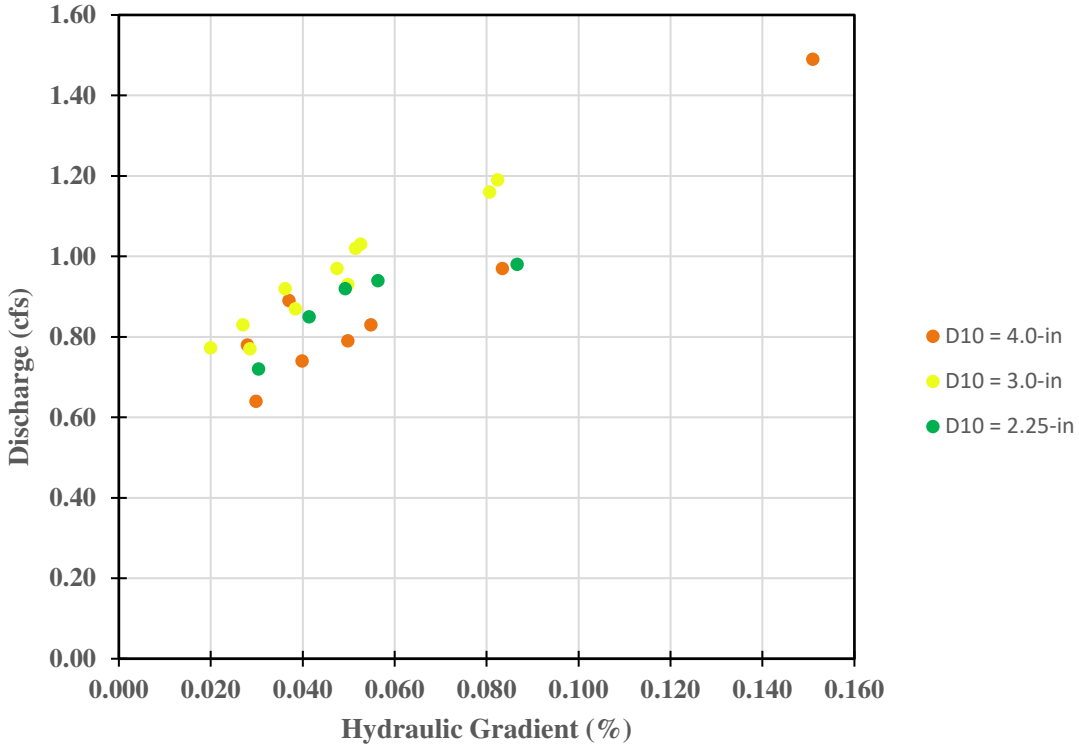

Figure 4-6 Discharge versus hydraulic gradient for different D_{10} values, current study data only

Figure 4-3 to 4-6 also reveal that there is an apparent effect due to different D_{50} and D_{10}, but this effect is not immediately apparent. Figure 4-5 reveals that as D_{10} increases, discharge increases. Parameters D_{50} and D_{10} do not appear trend with slope and discharge in the 2.25-in and 4.0-in rock sizes. For example, discharge values in tests A-1 to A-5, which have a D_{50} and D_{10} of 3.0-in and 2.25-in respectively, are both higher and lower than other tests with larger D_{50} and D_{10}. Adding a more diverse set of rock sizes and gradations along with steeper slopes may reveal the trend that is expected (i.e. positive relationship between D_{50} and D_{10} and discharge). For this set of tests, data is limited by the thin range of rock sizes from 2.25-in to 4.0-in. Figures 4-3 to 4-6 also reveal that other factors apart from rock D_{50} and D_{10} and bed slope may be affecting discharge.

Interstitial Velocity Results

Interstitial velocities can be described by either the local velocity or an average velocity based on continuity. As described in Chapter 1, the particle velocity is volatile and difficult to measure in the voids of a rock layer. To avoid skewed particle velocity data, multiple measurements are required to identify an appropriate description of velocity value(s) (i.e. describing by an average, max, min, etc.). Furthermore, installing instrumentation that will fit in the voids of the rock presents a challenge. Modern velocity instrumentation is generally too fragile or too large to use within a rock layer. Large instrumentation will disrupt the normal interstitial flow characteristics within the rock layer.

Velocities in this study were obtained using calculated velocity, V_c, as described earlier in Chapter 2. As mentioned in Chapter 3, a range of n_p were measured for each rock configuration. The maximum values in each range were used in V_c calculations shown in Table 3-4. Maximum values were chosen because the highest porosity value corresponded best with the actual porosity

in the gabion mattresses used for testing. Since rock was dumped into the flume, this created larger voids among the rock layer, thus having a higher porosity than if the rock was hand-placed. Figure 4-7 to Figure 4-10 show calculated velocity plots versus bed slope and hydraulic gradient. Data is color separated by different D_{50}'s or D_{10}'s.

Data in Figure 4-7 to Figure 4-10 are similar in shape to their discharge counterpart in Figure 4-3 to Figure 4-6. Plots of discharge and plots of calculated interstitial velocities are analogous since velocity is a scaled discharge value by area and porosity. Therefore, the same conclusions from the discharge data can be repeated for the velocity data:

There is a positive linear relationship between bed slope/hydraulic gradient and V_c. Also, the plots show that the effect of D_{50} and D_{10} are still not readily discernible. Generally, the smaller the pores and therefore a higher roughness and slower velocity. Also, smaller pores in the rock layer create a longer flow path than are present for larger rock with larger pores. Figure 4-9 reveals that as D_{10} increases, V_c increases. Rock with a small D_{10} (blue in Figure 4-9) strongly supports this conclusion. However, D_{50} and D_{10} still do not appear to have a trend with slope and velocity in the 2.25-in and 4.0-in rock. The example involving tests A-1 to A-5 mentioned in the previous section is repeated for velocity, where now velocity values for a D_{50} and D_{10} of 3.0-in and 2.25-in, respectively, are both higher and lower than other tests with larger D_{50} and D_{10}. Again, a broader set of rock sizes and gradations may reveal the trend that is expected (positive relationship between D_{50} and D_{10} and velocity).

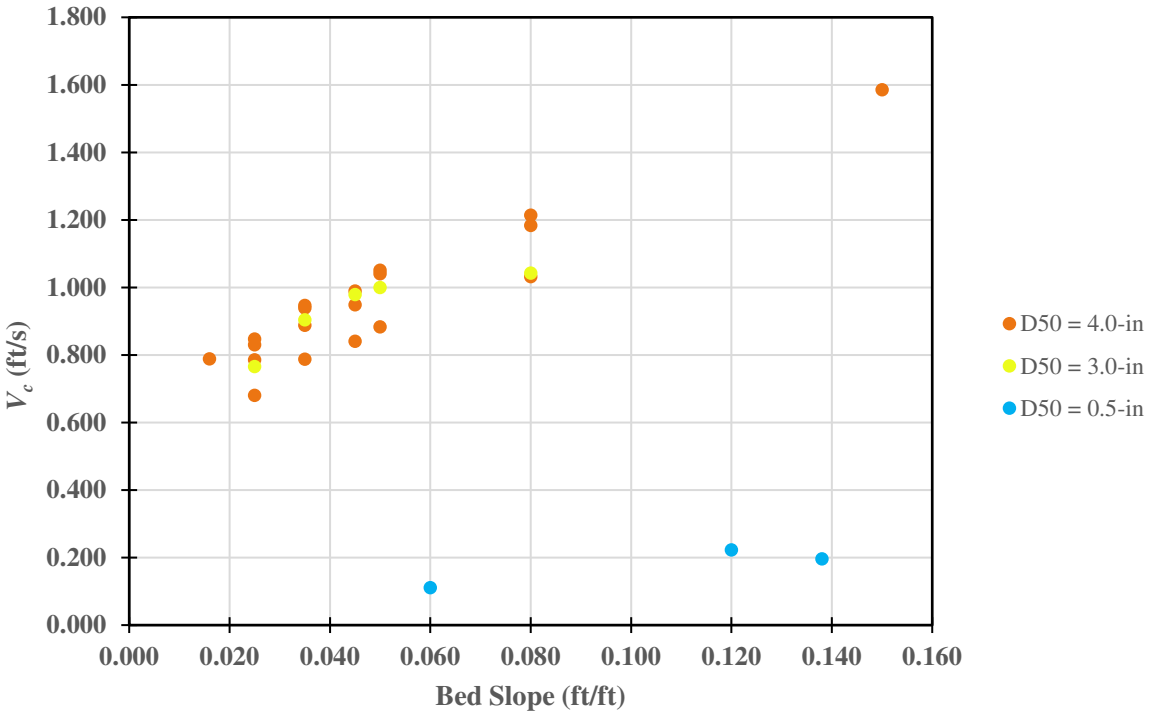

Figure 4-7 Calculated velocity versus bed slope for different D_{50} values, current study data only

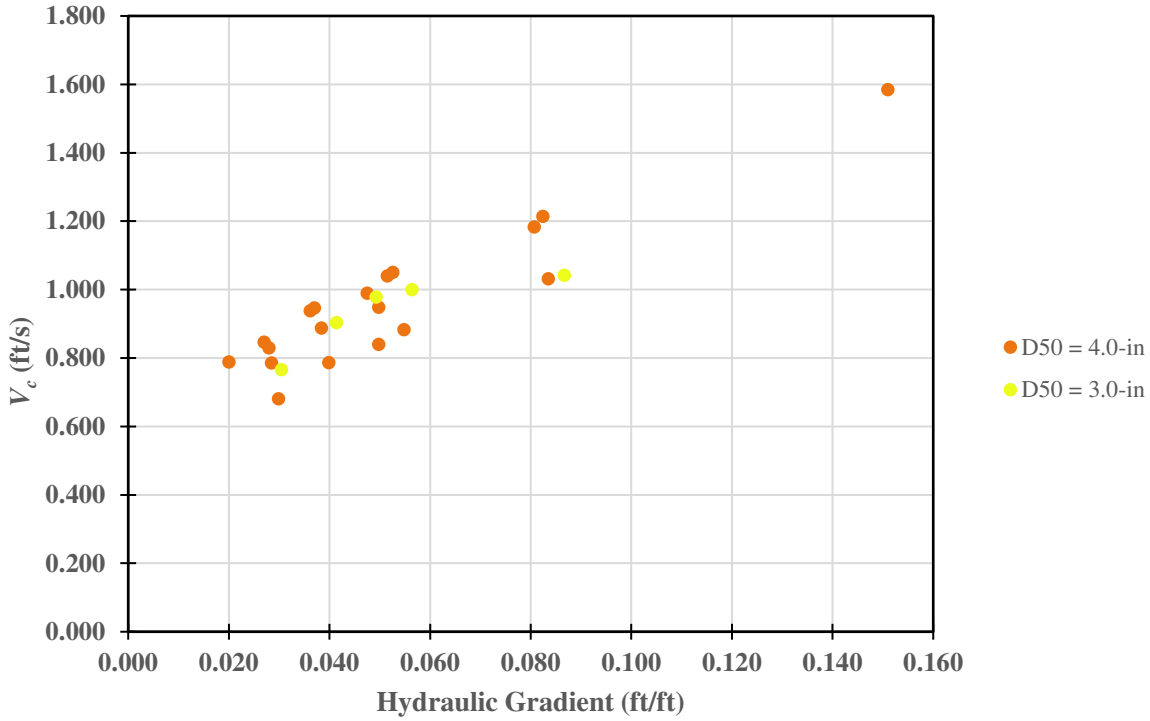

Figure 4-8 Calculated velocity versus hydraulic gradient for different D_{50} values, current study data only

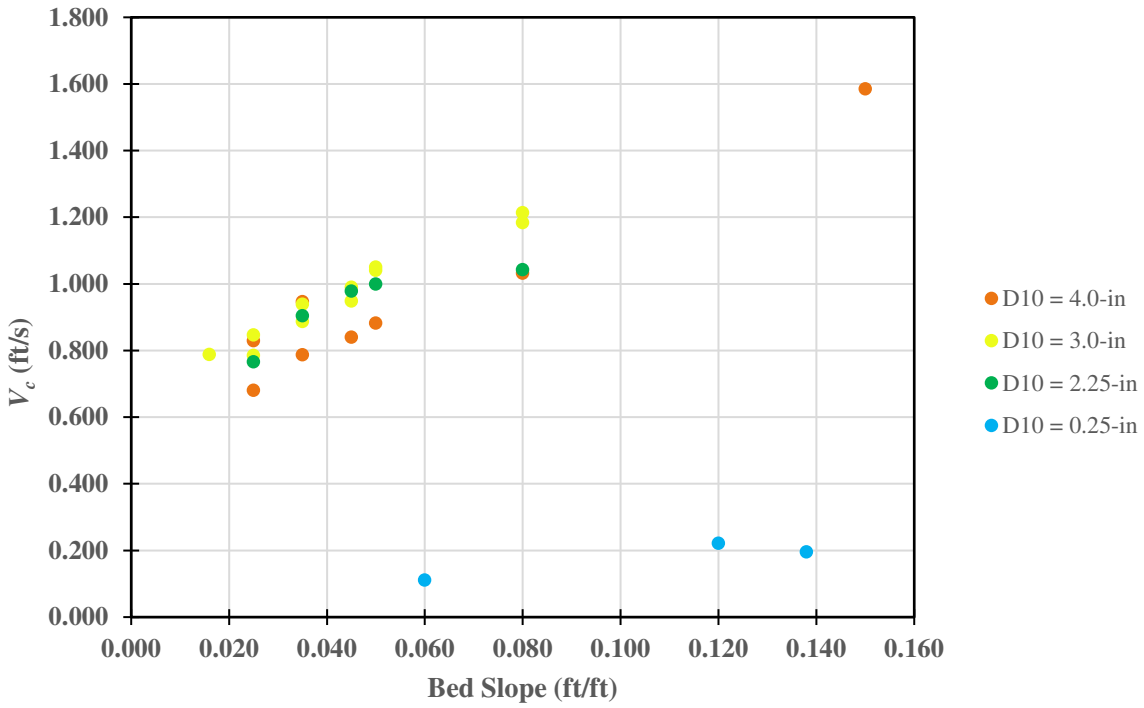

Figure 4-9 Calculated velocity versus bed slope for different D_{10} values, current study data only

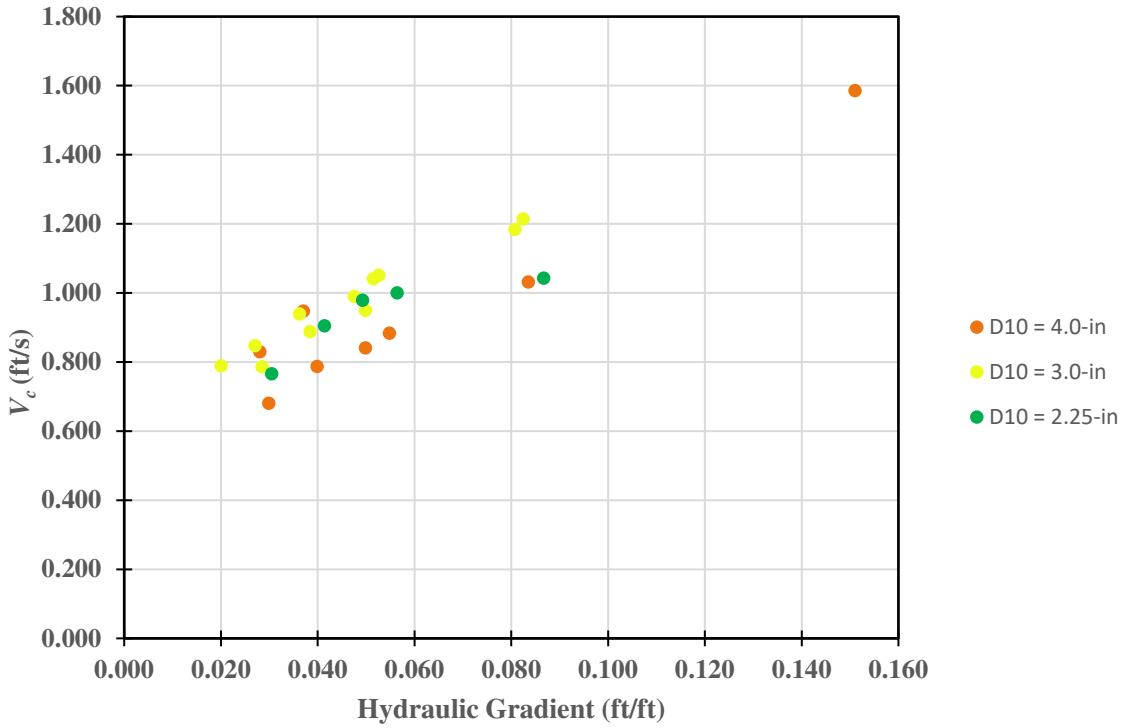

Figure 4-10 Calculated velocity versus hydraulic gradient for different D_{10} values, current study data only

Discharge and Calculated Velocity Analyses Using Current and Past Data

Data from Abt et al. (1987, 1988) were compiled with data from the current study and are shown in Figure 4-11 to Figure 4-14. Not all data from Abt et al. (1987, 1988) were used in these analyses. Only results from tests using the indoor flume were deemed compatible with the data in the current study due to experimental difference. Similar analyses as the preceding sections were performed to further evaluate the effect of D_{50} and D_{10} on interstitial discharge and velocity. Discharge data from Abt et al. (1987, 1988) were converted to a discharge per square foot of rock for direct comparison.

The addition of the indoor flume data from Abt et al. (1987, 1988) provide the range of rock sizes to more thoroughly analyze the significance of D_{50} and D_{10} on discharge potential and interstitial flow velocity. A visual analysis of Figure 4-11 to Figure 4-14 shows that smaller rock is associated with less discharge and slower flow velocity.

Influence of bed slope on discharge and flow velocity is also reinforced by Figures 4-11 to 4-14. Most rock sizes in these figures display a positive linear relationship between discharge or velocity and bed slope. Figures of hydraulic gradient on the x-axis in substitute of bed slope were not used in these analyses due to the redundancy illustrated in the previous section and because this parameter is not provided by Abt et al. (1987, 1988). Hydraulic gradient is also a parameter that is difficult to estimate for a design engineer. For these reasons, hydraulic gradient is not considered for equations generated in this study to predict interstitial discharge and interstitial velocity. Referring to Abt et al. (1987, 1988), C_u was concluded to be a parameter that significantly influences discharge and interstitial velocity. Current study data did not have a range of C_u values to properly interpret the significance of varying this parameter. C_u values in

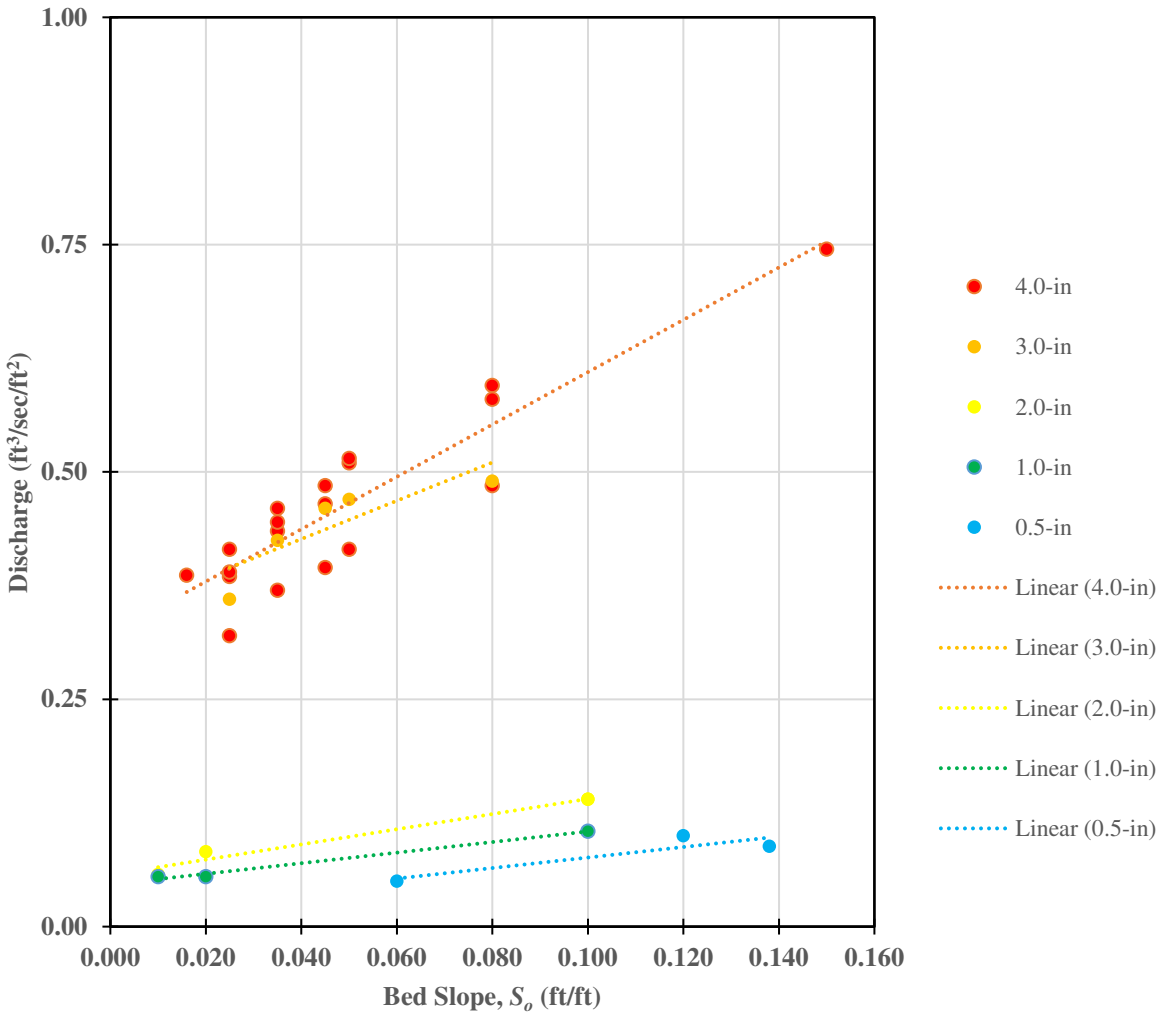

Figure 4-11 Plots and associated trendlines of measured discharge per square foot of rock vs bed slope by D_{50}; data from current study and Abt et al. (1987, 1988) indoor flume tests

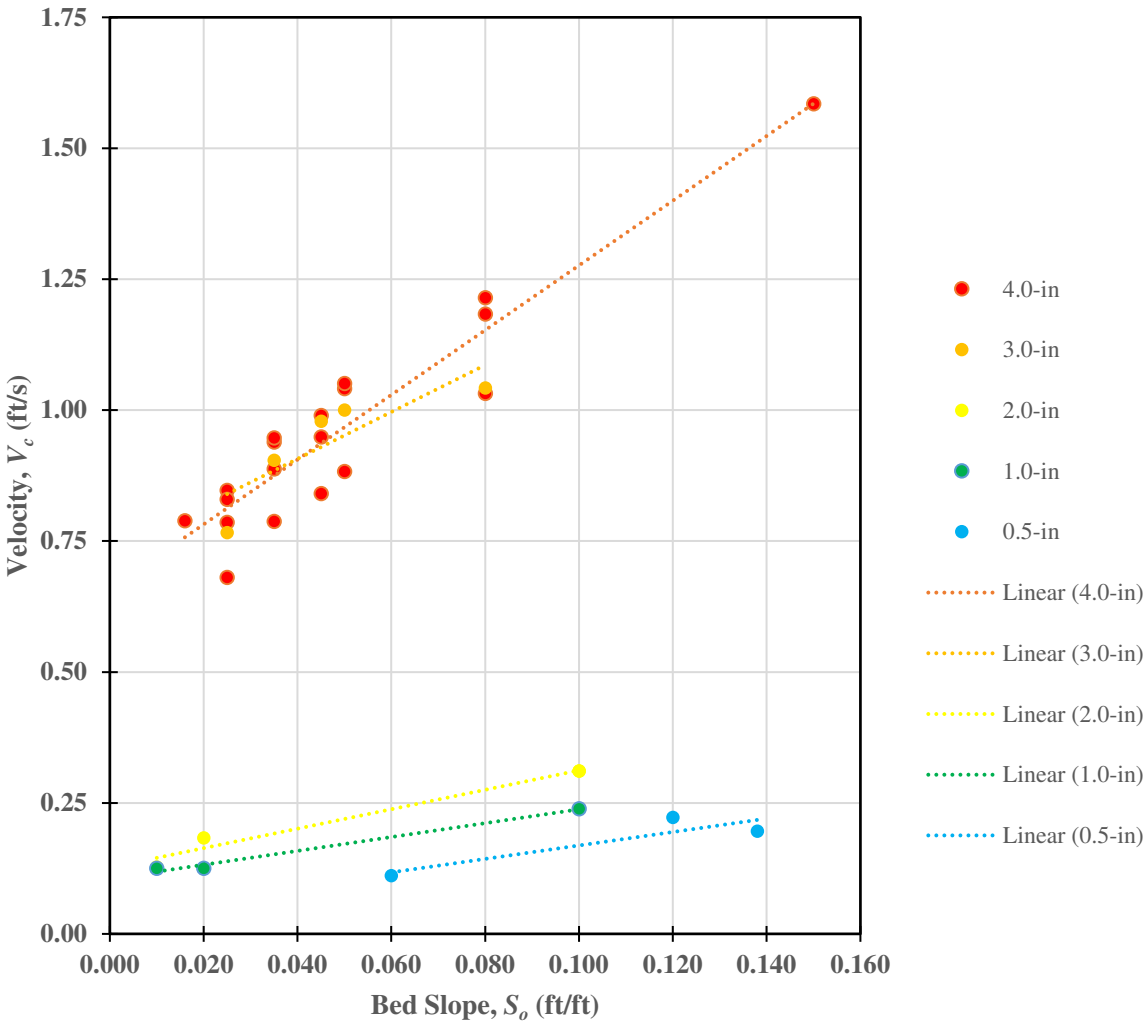

Figure 4-12 Plots and associated trendlines of calculated test velocity vs bed slope by D_{50}; data from current study and Abt et al. (1987, 1988) indoor flume tests

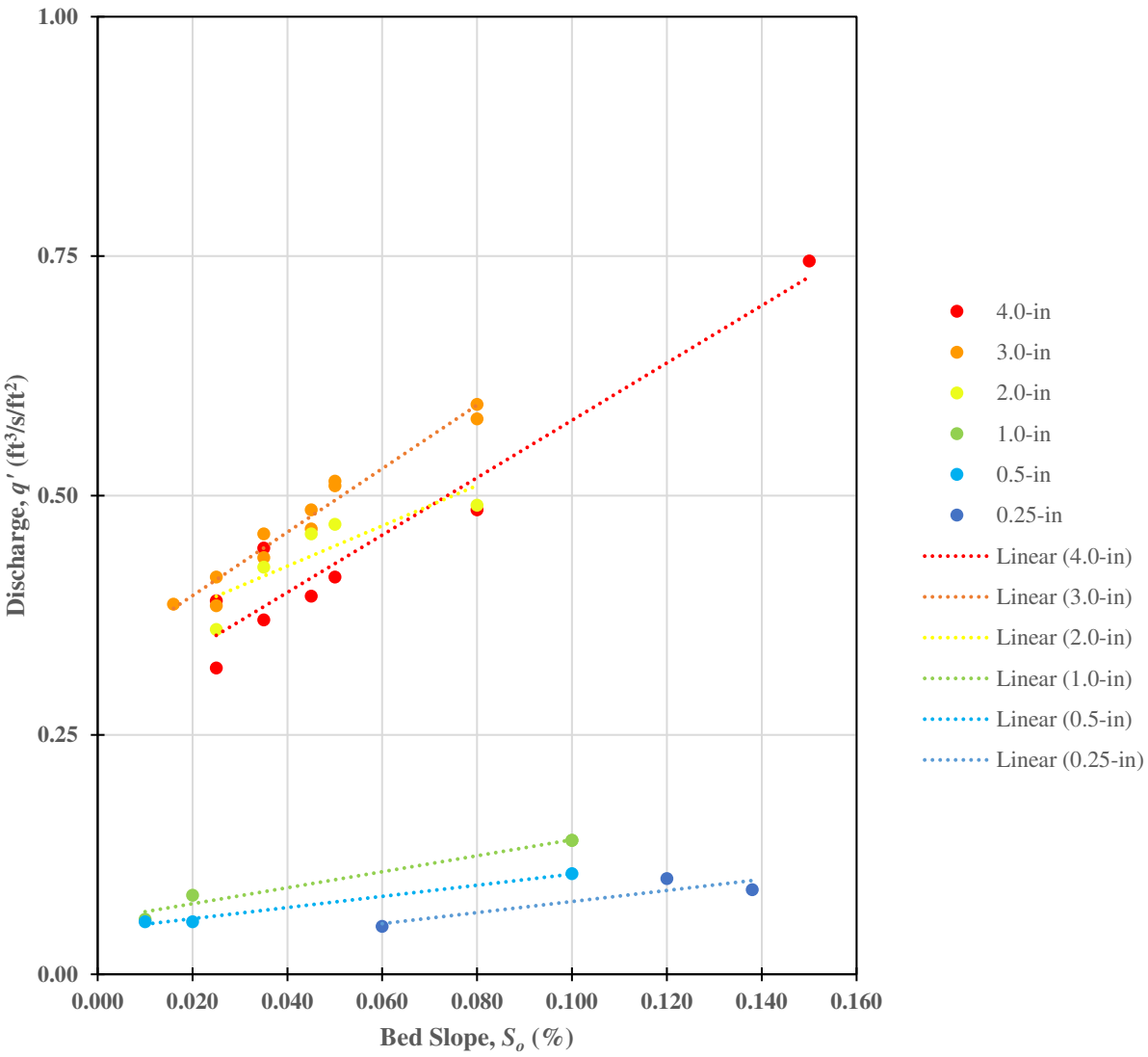

Figure 4-13 Plots and associated trendlines of measured unit discharge per square foot of rock vs bed slope by D_{10}; data from current study and Abt et al. (1987, 1988) indoor flume tests

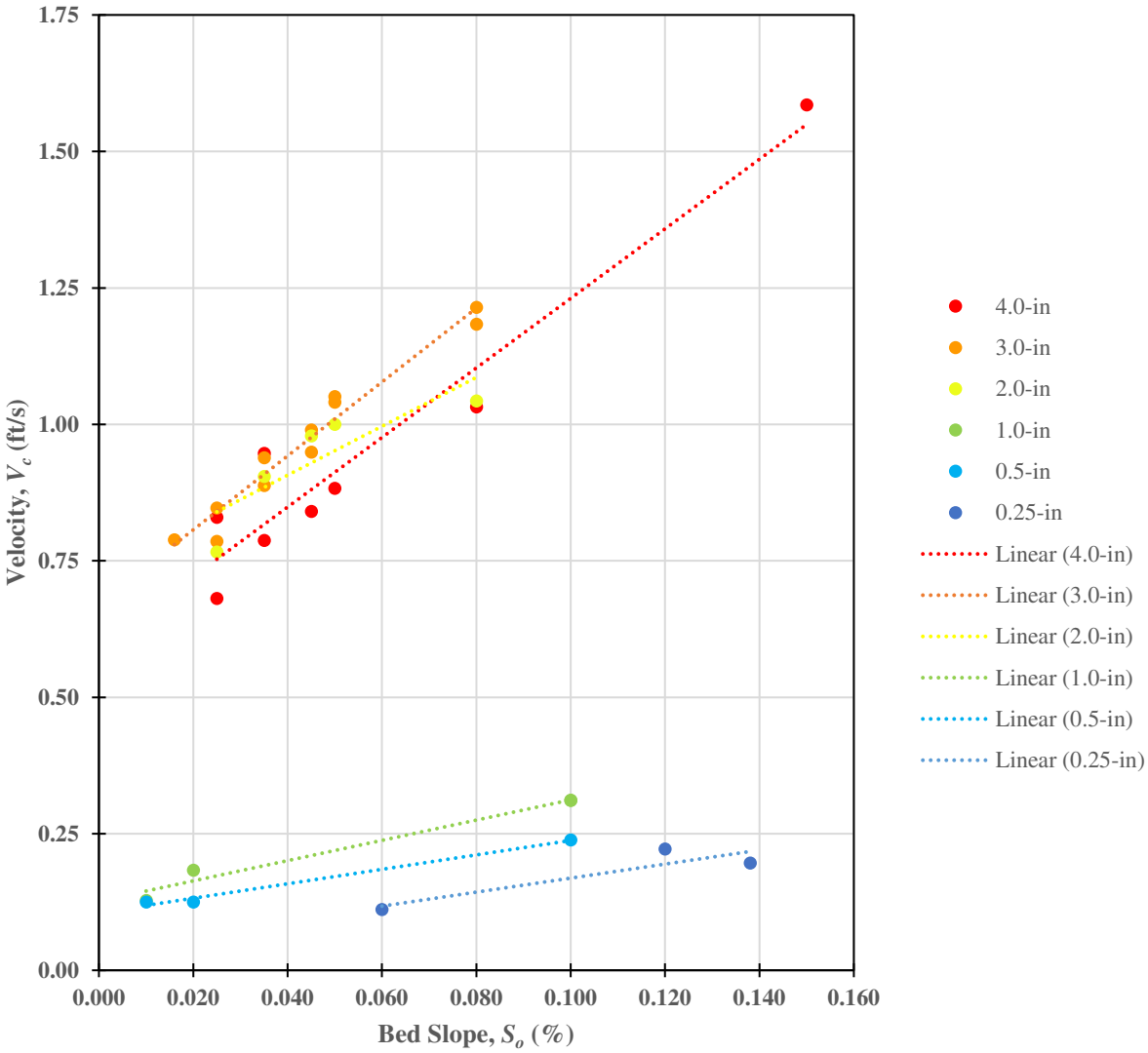

Figure 4-14 Plots and associated trendlines of calculated test velocity vs bed slope by D_{10}; data from current study and Abt et al. (1987, 1988) indoor flume tests

the Abt et al. (1987, 1988) included 1.62, 1.75, 2.10, 2.15, 2.30, and 4.0, whereas the values in the current study included 1.0, 1.5, and 2.0. Abt et al. (1987, 1988) was able to isolate C_u for analysis and determined a higher C_u correlated with less potential discharge and less velocity.

Porosity was deemed inapplicable to this study, as this parameter would also be difficult to measure or obtain for a design engineer. Therefore, porosity is not included in the development of equations generated in this study to predict discharge and flow velocity.

Parameters used in the development of a new equation to estimate interstitial flow velocity and discharge include rock D_{50} and D_{10}, C_u, and S_o. All four parameters are proven to be significant in estimation of interstitial flow velocity and discharge, and all can be easily obtainable by a design engineer.

CHAPTER 5. EQUATION DEVELOPMENT TO ESTIMATE INTERSTITIAL VELOCITY AND DISCHARGE

Two equations are developed to estimate interstitial velocity and discharge. A form for the equation was chosen and a multivariate power regression was performed for the equation development.

Equation Form

Five parameters (D_{50}, $D_{10,}$ C_u, g, and S_o) were used to develop the design (predictive) equations for estimating interstitial velocity and unit discharge. Parameters representing the new estimated interstitial velocity and interstitial discharge are V_{ik} and q_{ik}, respectively. Current study data and data from the indoor testing by Abt et al. (1987, 1988) only are used in the new equation development. As described in Chapter 4, the experimental setup and procedure of the indoor flume tests performed by Abt were the exact same as the experimental setup of the tests in the current study. Therefore, the two data sets are combined for equation development. Based on visual inspection of the data, a power function was selected for equation development, and a multivariate nonlinear regression is used to develop power coefficients.

Multiple equation configurations were taken into consideration. After a series of regression trials with each configuration, a single configuration was chosen for both velocity and discharge. Appendix A summarizes the configurations tested and associated regression statistics used to determine which produced the best results. The following section describes the statistical program used for this regression.

Equation 10 and Equation 11 present the developed equation structure to estimate velocity and discharge per square foot of rock, respectively, of interstitial flow in aggregate rock.

Four terms $g \bullet D_{50}$, $g \bullet D_{10}$, C_u, and S_o are assigned a unique power coefficient, and a single scalar coefficient is multiplied by the product of all terms. D_{50} and D_{10} are in feet, acceleration due to gravity is in ft/s^2, and bed slope is in ft/ft. C_u is dimensionless.

$$V_{ik} = a(gD_{50})^b(gD_{10})^c C_u^d S_o^f \tag{10}$$

$$q_{ik} = l(gD_{50})^m(gD_{10})^n C_u^o S_o^p \tag{11}$$

where:

V_{ik} = average interstitial velocity (ft/sec)

q_{ik} = discharge per square foot of rock; (ft^3/sec/ft^2)

a, b, c, d, f, l, m, n, o, p = coefficients (dimensionless)

Regression Analysis

A multivariate nonlinear power regression was completed to find coefficients *a*, *b*, *c*, *d*, and *f* for the interstitial velocity and *l*, *m*, *n*, *o*, *p* for discharge. A data analysis software package XLSTAT is used for regression analyses. XLSTAT is a downloadable extension for Microsoft Excel and can perform regression using a statistical based analysis to calculate coefficients desired.

Inputs required in this regression analysis included the structure of the equation (i.e. designating the location for each variable and coefficient in the expression) and the table of values for each dependent variable with the associated independent variable. Equation 12 provides the general form of the structure inputted into XLSTAT.

Table 5-1 summarizes the data format inputted into the program for analysis. Results of the regressions are presented in the following sections for V_{ik} and q_{ik}.

$$Y = p_{r1}(gX_1)^{pr2}(gX_2)^{pr3}X_3^{pr4}X_4^{pr5} \tag{12}$$

Table 5-1 Data table inputted into regression program

		X_1	X_2	X_3	X_4	Y	Y
Study	**Test ID**	D_{50}	D_{10}	C_u	S_o	V_c	q'
	Flume-No.	Feet	Feet	-	ft/ft	ft/s	$ft^3/s/ft^2$
Abt	6 I	0.083	0.050	1.75	0.010	0.13	0.06
Abt	7 I	0.083	0.050	1.75	0.020	0.13	0.06
Abt	9 I	0.083	0.050	1.75	0.100	0.24	0.11
Abt	4 I	0.183	0.092	2.09	0.010	0.13	0.06
Abt	3 I	0.183	0.092	2.09	0.020	0.18	0.08
Abt	10 I	0.183	0.092	2.09	0.100	0.31	0.14
Abt	11 I	0.183	0.092	2.09	0.100	0.31	0.14
This study	A-1	0.250	0.188	1.5	0.025	0.77	0.36
This study	A-2	0.250	0.188	1.5	0.035	0.90	0.43
This study	A-3	0.250	0.188	1.5	0.045	0.98	0.46
This study	A-4	0.250	0.188	1.5	0.050	1.00	0.47
This study	A-5	0.250	0.188	1.5	0.080	1.04	0.49
This study	A-6	0.333	0.250	1.5	0.016	0.79	0.39
This study	A-7	0.333	0.250	1.5	0.025	0.79	0.39
This study	A-8	0.333	0.250	1.5	0.025	0.85	0.42
This study	A-9	0.333	0.250	1.5	0.035	0.89	0.44
This study	A-10	0.333	0.250	1.5	0.035	0.94	0.46
This study	A-11	0.333	0.250	1.5	0.045	0.95	0.47
This study	A-12	0.333	0.250	1.5	0.045	0.99	0.49
This study	A-13	0.333	0.250	1.5	0.050	1.04	0.51
This study	A-14	0.333	0.250	1.5	0.050	1.05	0.52
This study	A-15	0.333	0.250	1.5	0.080	1.21	0.60
This study	A-16	0.333	0.250	1.5	0.080	1.18	0.58
This study	A-17	0.333	0.333	1.0	0.025	0.68	0.32
This study	A-18	0.333	0.333	1.0	0.025	0.83	0.39
This study	A-19	0.333	0.333	1.0	0.035	0.79	0.37
This study	A-20	0.333	0.333	1.0	0.035	0.95	0.45
This study	A-21	0.333	0.333	1.0	0.045	0.84	0.40
This study	A-22	0.333	0.333	1.0	0.050	0.88	0.42
This study	A-23	0.333	0.333	1.0	0.080	1.03	0.49
This study	B-1	0.333	0.333	1.0	0.150	1.59	0.75
This study	C-1	0.042	0.021	2.0	0.060	0.11	0.05
This study	C-2	0.042	0.021	2.0	0.120	0.22	0.10
This study	C-3	0.042	0.021	2.0	0.138	0.20	0.09

Regression Results – Interstitial Velocity

Equation 13 is the resulting equation from the interstitial velocity regression, and Table 5-2 and Table 5-3 present the goodness of fit statistics of the regression and the resulting coefficient values, respectively.

$$V_{ik} = 1.287(gD_{50})^{-7.863}(gD_{10})^{8.194}C_u^{6.016}S_o^{0.360} \quad (13)$$

Interstitial velocity results from the regression are presented in Table 5-4, which displays the measured velocity, estimated velocity from Equation 13, the residual error between the two, and the associated percent error. Error and percent error averages are displayed at the bottom of the table. Figure 5-1 displays a plot the regression results.

Table 5-2 Interstitial velocity regression goodness of fit statistics

Statistic	Value
Observations	34
Degrees of freedom	29
R^2	0.972
Best fit line slope	0.995
Mean error (ft/s)	± 0.052
Mean error (%)	± 10.24
Sum of square errors	0.138
Mean square error	0.005
Iterations	7

Table 5-3 Interstitial velocity regression coefficient values

Parameters	Value	Standard error
a	1.287	0.341
b	-7.863	1.026
c	8.194	0.951
d	6.016	0.683
f	0.360	0.028

Table 5-4 Data table of results from developed interstitial velocity equation

Study	**Test ID**	V_c ft/s	**Pred. *V*** ft/s	**Residual** ft/s	**Percent Error** %
Abt	6 I	0.125	0.150	-0.025	20.1
Abt	7 I	0.125	0.193	-0.068	54.1
Abt	9 I	0.239	0.344	-0.105	44
Abt	4 I	0.128	0.127	0.001	0.4
Abt	3 I	0.183	0.163	0.020	10.9
Abt	10 I	0.311	0.291	0.020	6.4
Abt	11 I	0.311	0.291	0.020	6.4
This study	A-1	0.766	0.739	0.027	3.5
This study	A-2	0.904	0.834	0.070	7.8
This study	A-3	0.979	0.913	0.066	6.7
This study	A-4	1.000	0.948	0.052	5.2
This study	A-5	1.043	1.122	-0.080	7.7
This study	A-6	0.789	0.692	0.097	12.3
This study	A-7	0.786	0.812	-0.027	3.4
This study	A-8	0.847	0.812	0.034	4.1
This study	A-9	0.888	0.917	-0.029	3.3
This study	A-10	0.939	0.917	0.022	2.3
This study	A-11	0.949	1.004	-0.055	5.8
This study	A-12	0.990	1.004	-0.014	1.4
This study	A-13	1.041	1.042	-0.002	0.2
This study	A-14	1.051	1.042	0.009	0.8
This study	A-15	1.214	1.234	-0.020	1.7
This study	A-16	1.184	1.234	-0.051	4.3
This study	A-17	0.681	0.748	-0.068	9.9
This study	A-18	0.830	0.748	0.081	9.8
This study	A-19	0.787	0.845	-0.057	7.3
This study	A-20	0.947	0.845	0.102	10.8
This study	A-21	0.840	0.925	-0.084	10
This study	A-22	0.883	0.960	-0.077	8.7
This study	A-23	1.032	1.137	-0.105	10.2
This study	B-1	1.585	1.425	0.160	10.1
This study	C-1	0.111	0.114	-0.003	2.6
This study	C-2	0.222	0.146	0.076	34.2
This study	C-3	0.196	0.154	0.042	21.6
average				0.052	10.24

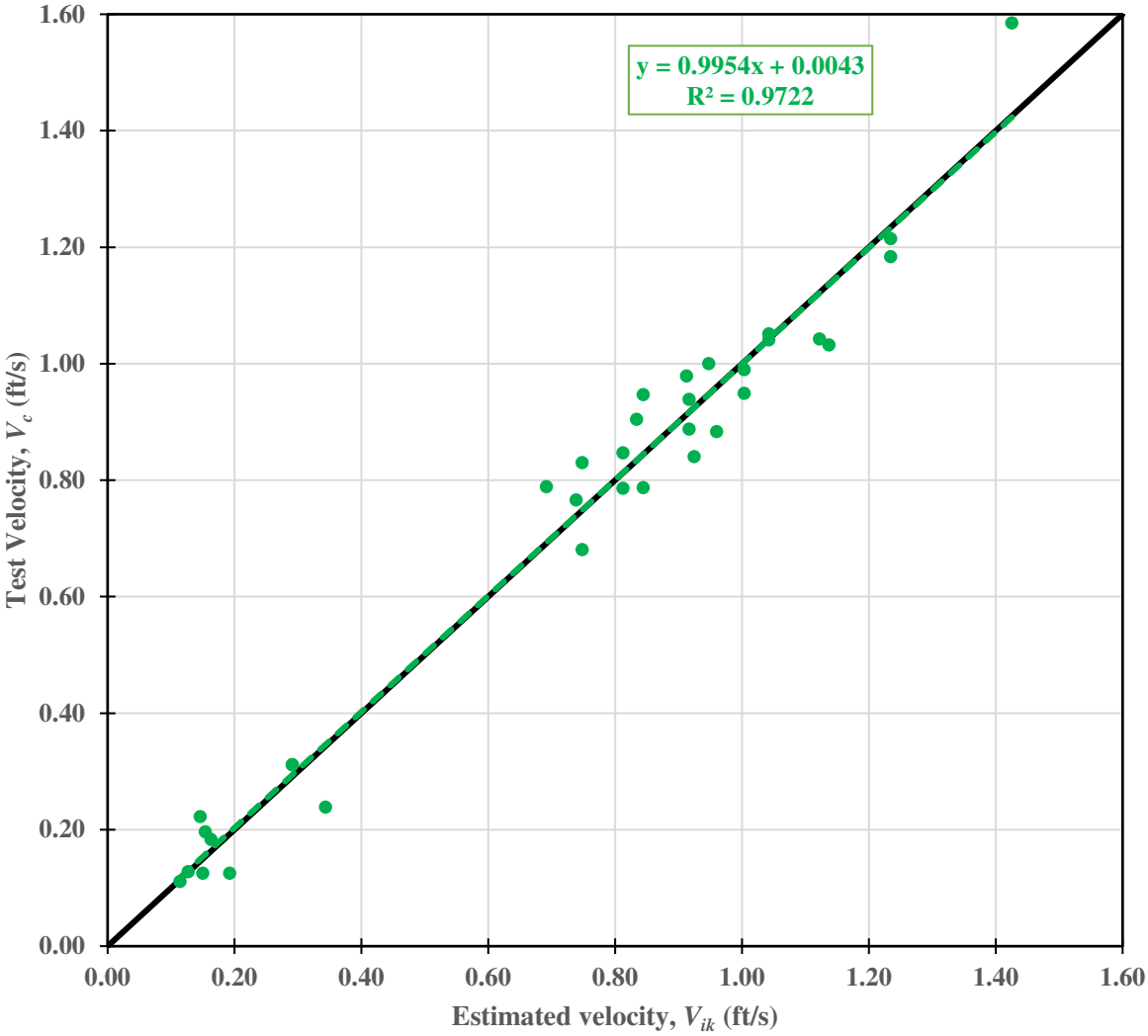

Figure 5-1 Measured versus estimated, based on output from Equation 13, velocities

Regression Results –Discharge

Equation 14 is the developed equation from the unit discharge regression using both sets of data, and Table 5-5 and Table 5-6 summarize the goodness of fit statistics of the regression and the resulting power coefficients, respectively.

$$q_{ik} = 0.483(gD_{50})^{-7.852}(gD_{10})^{8.275}C_u^{6.163}S_o^{0.357} \quad (14)$$

Discharge results from the regression are presented in Table 5-7. Error and percent error averages are tabulated at the bottom of the table. Figure 5-2 contains a plot the regression results.

Table 5-5 Unit discharge regression goodness of fit statistics

Statistic	Value
Observations	34
Degrees of freedom	29
R^2	0.974
Best fit line slope	0.994
Mean error ($ft^3/s/ft^2$)	± 0.024
Mean error (%)	± 10.21
Sum of square errors	0.030
Mean square error	0.001
Iterations	8

Table 5-6 Interstitial velocity regression coefficient values

Parameters	Value	Standard error
l	0.483	0.128
m	-7.852	1.016
n	8.275	0.944
o	6.163	0.678
p	0.357	0.027

Table 5-7 Data table of results from developed unit discharge equation

Study	**Test ID**	***q'*** $ft^3/s/ft^2$	**Pred. *q'*** $ft^3/s/ft^2$	**Residual** $ft^3/s/ft^2$	**Percent Error** %
Abt	6 I	0.055	0.065	-0.010	18.1
Abt	7 I	0.055	0.083	-0.028	51.3
Abt	9 I	0.105	0.148	-0.043	40.9
Abt	4 I	0.058	0.060	-0.002	4.2
Abt	3 I	0.083	0.077	0.006	7.0
Abt	10 I	0.140	0.136	0.004	2.6
Abt	11 I	0.140	0.136	0.004	2.6
This study	A-1	0.360	0.351	0.009	2.4
This study	A-2	0.425	0.396	0.029	6.7
This study	A-3	0.460	0.434	0.026	5.7
This study	A-4	0.470	0.450	0.020	4.2
This study	A-5	0.490	0.533	-0.043	8.7
This study	A-6	0.387	0.338	0.048	12.4
This study	A-7	0.385	0.397	-0.012	3.1
This study	A-8	0.415	0.397	0.018	4.4
This study	A-9	0.435	0.448	-0.013	2.9
This study	A-10	0.460	0.448	0.012	2.7
This study	A-11	0.465	0.490	-0.025	5.3
This study	A-12	0.485	0.490	-0.005	1.0
This study	A-13	0.510	0.508	0.002	0.3
This study	A-14	0.515	0.508	0.007	1.3
This study	A-15	0.595	0.601	-0.006	1.1
This study	A-16	0.580	0.601	-0.021	3.7
This study	A-17	0.320	0.353	-0.033	10.2
This study	A-18	0.390	0.353	0.037	9.6
This study	A-19	0.370	0.398	-0.028	7.4
This study	A-20	0.445	0.398	0.047	10.7
This study	A-21	0.395	0.435	-0.040	10.1
This study	A-22	0.415	0.452	-0.037	8.8
This study	A-23	0.485	0.534	-0.049	10.1
This study	B-1	0.745	0.669	0.076	10.2
This study	C-1	0.050	0.046	0.004	7.4
This study	C-2	0.100	0.059	0.041	40.7
This study	C-3	0.088	0.062	0.026	29.4
average				0.024	10.21

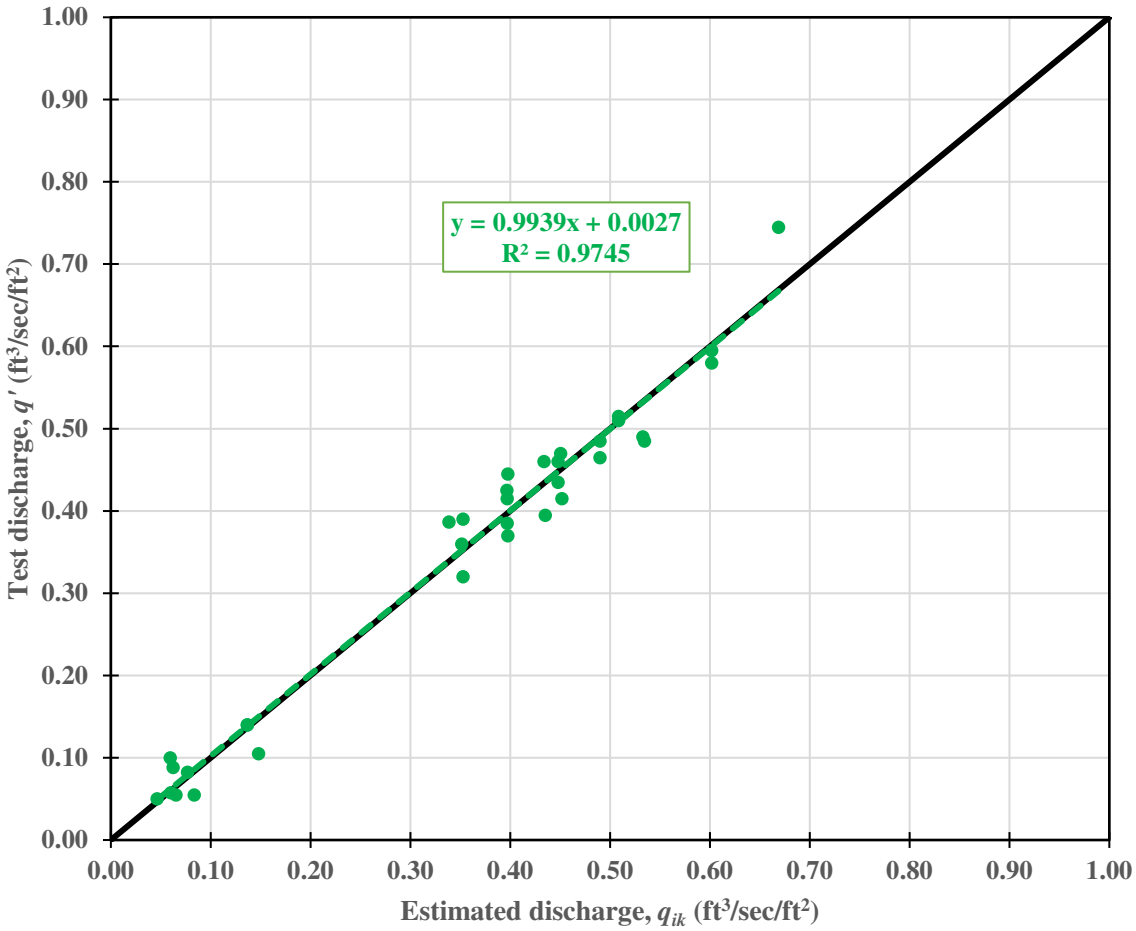

Figure 5-2 Measured versus estimated, using Equation 14, interstitial unit discharge per ft^2 rock

Regression Results – Conclusions

Results of this study illustrate that Equation 13 and Equation 14 sufficiently estimate average interstitial velocity and interstitial discharge from both the current study data and the Abt et al. (1987, 1988) indoor flume tests. Goodness of fit analyses for both Equation 13 and Equation 14 yield R^2 above 0.97, and based on a visual analysis from Figure 5-1 and Figure 5-2, best fit lines closely resemble a line of perfect correlation in the range of velocity and discharge values.

Additionally, Equations 13 and 14 provide more accurate results than the equations previously developed by Abt et al. (1987, 1988) and are better suited for use by a design engineer. To illustrate this argument, goodness of fit statistics are tabulated in Table 5-8 and a visual comparison of the correlations between the performance of Abt et al. (1987, 1988) equations and Equation 13 and Equation 14 developed in this study are shown in Figure 5-3 and Figure 5-4.

Table 5-8 Goodness of fit statistics for Abt and current study (Keene) equations

Parameter Measured vs Estimated	Input data	Equation	Equation Number	R^2	Line of Best Fit Equation
Velocity	Abt	Abt V_{i1}	(7)	0.796	1.03x + 0.021
Velocity	Abt	Abt V_{i2}	(8)	0.731	0.96x + 0.132
Discharge	Abt	Abt q^*	(9)	0.690	1.02x + 0.006
Velocity	Keene	Abt V_{i1}	(7)	0.754	1.38x + 0.150
Velocity	Keene	Abt V_{i2}	(8)	0.694	0.78x + 0.238
Discharge	Keene	Abt q^*	(9)	0.620	1.02x + 0.145
Velocity	Keene & Abt indoor	Abt V_{i1}	(7)	0.718	1.75x - 0.008
Velocity	Keene & Abt indoor	Abt V_{i2}	(8)	0.807	1.81x - 0.051
Discharge	Keene & Abt indoor	Abt q^*	(9)	0.669	1.36x + 0.056
Velocity	**Keene & Abt indoor**	**Keene V_{ik}**	**(13)**	**0.972**	**0.99x + 0.004**
Discharge	**Keene & Abt indoor**	**Keene q_{ik}**	**(14)**	**0.974**	**0.99x + 0.003**

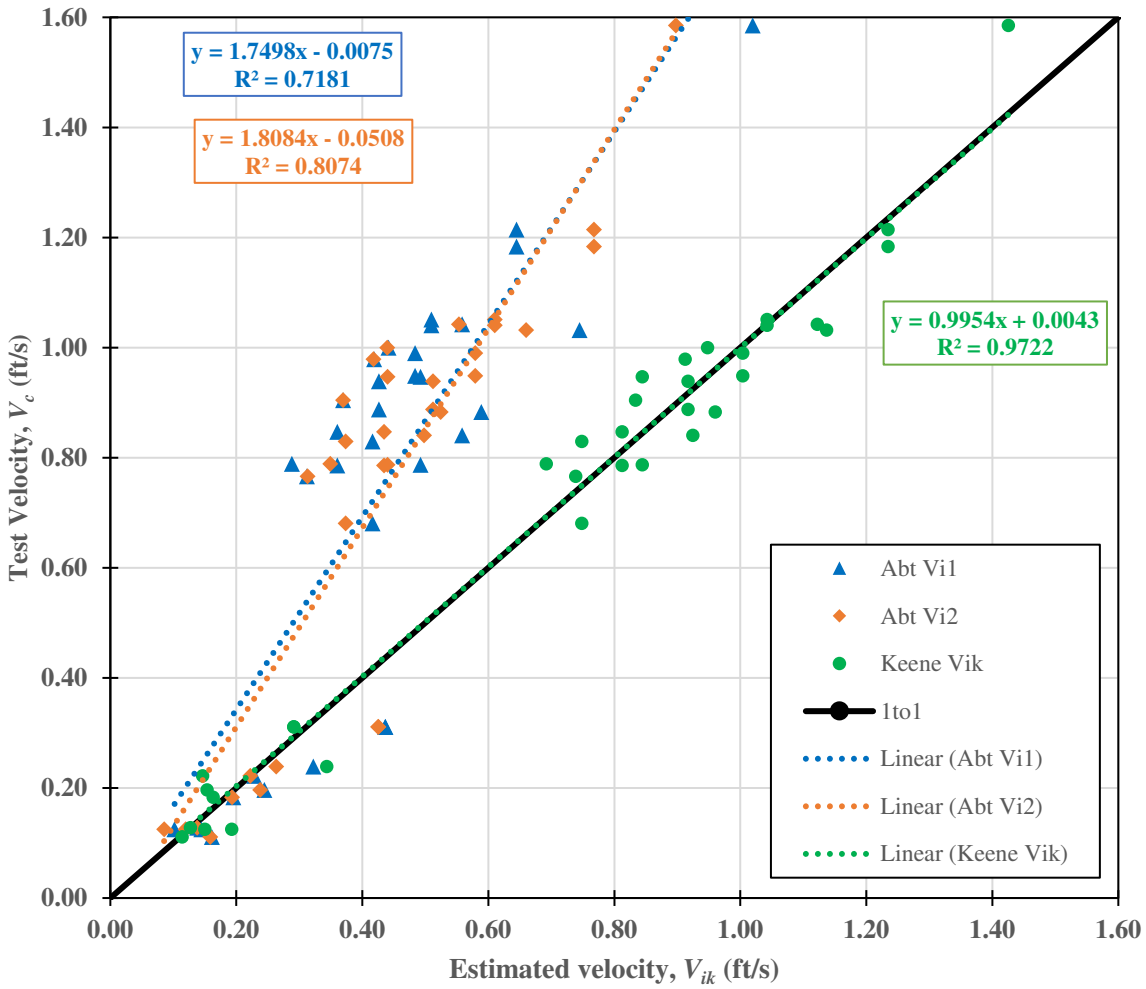

Figure 5-3 Comparison of measured versus predicted velocities from equations developed by Abt et al. (1987, 1988) V_{i1} and V_{i2} equations, and Equation 13 of this study

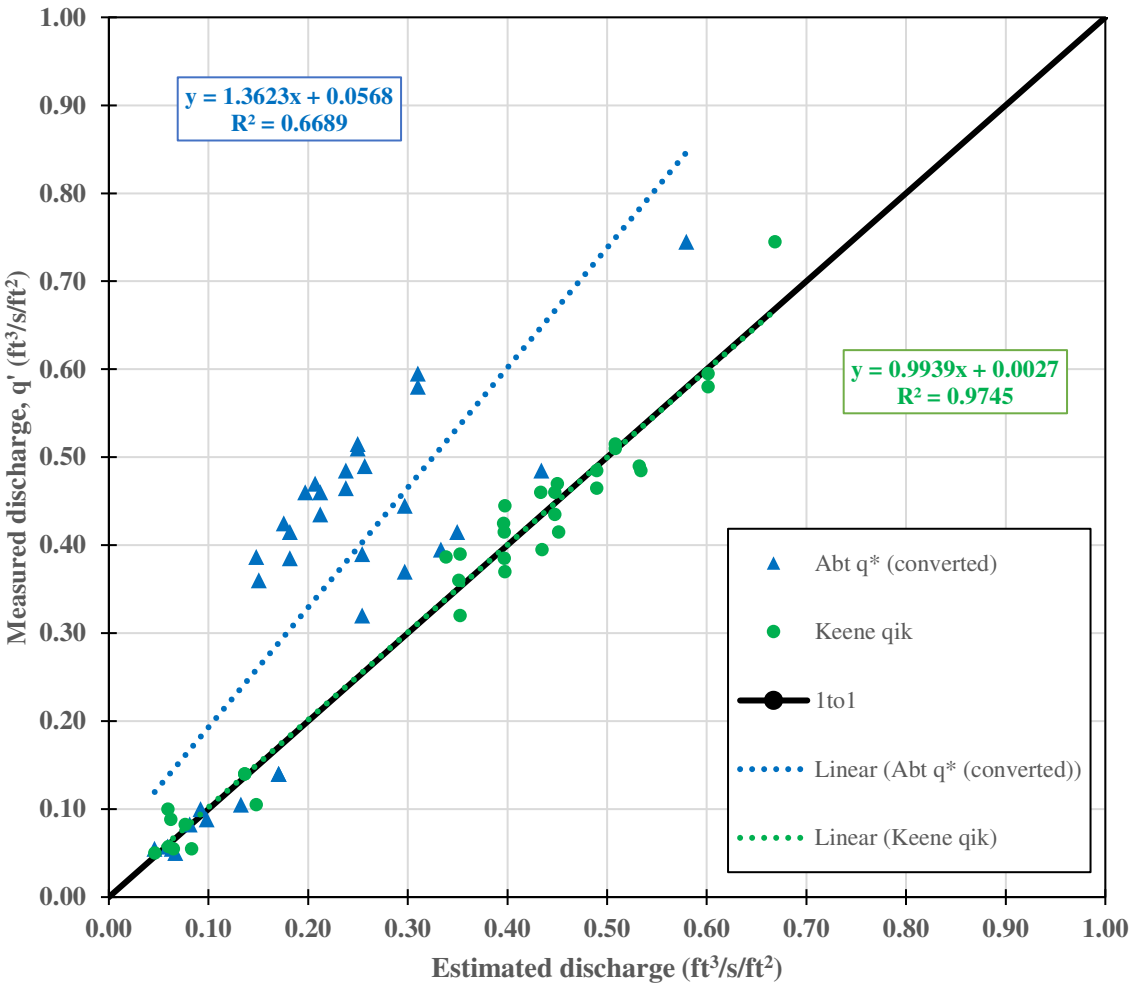

Figure 5-4 Comparison of measured versus predicted discharge from equations developed by Abt et al. (1987, 1988) q* equations (converted to q'), and Equation 13 of this study

Equation 13 improves upon Abt et al. (1987, 1988) equations V_{i1} and V_{i2} (Equation 7 and Equation 8, respectively) for estimating average interstitial velocity. Goodness of fit statistics improve from Equation 8 to Equation 13. R^2 is higher and the best fit line is nearly a perfect correlation in the Equation 13 regression analysis.

Equation 14 also improves upon Equation 9 as a design equation to estimate interstitial discharge. The goodness of fit statistics also convincingly reveals an improvement; both the Abt et al. (1987, 1988) equation and Equation 14 estimate discharge well considering both sets of data. However, by referring to Figure 5-4, a visual analysis reveals that Equation 9 underestimates discharge for almost all measured values, whereas predicted values from Equation 14 are nearly a perfect correlation with the measured values.

In addition to the quantitative and visual analyses presented previously, Equation 13 and Equation 14 are better suited for design use based on the availability of the input parameters in the equations. Developing empirical predictive equations to include only parameters typically easy to obtain for an engineer, Equation 13 and Equation 14 are more conducive to design use.

Guidelines for use of Equation 13 and Equation 14 in design, including limitations, recommendations, and best applications are presented in the Chapter 6.

CHAPTER 6. RECOMMENDATIONS AND CONCLUSIONS

Limitations and recommendations on the design use of Equation 13 and Equation 14 are described in this chapter.

$$V_{ik} = 1.287(gD_{50})^{-7.863}(gD_{10})^{8.194}C_u^{6.016}S_o^{0.360} \quad (13)$$

$$q_{ik} = 0.483(gD_{50})^{-7.852}(gD_{10})^{8.275}C_u^{6.163}S_o^{0.357} \quad (14)$$

Limitations of Use

Equation 13 and Equation 14 have limitations for use in estimating interstitial velocity and discharge in hydraulic engineering design applications. Rock properties and other testing parameters used in the experimental program for this study and Abt et al. (1987, 1988) indoor study set the range of use for the equations. Application of Equations 13 and 14 were developed using rock sizes from ¼ inch to 5 inches in nominal diameter, C_u from 1.0 to 2.1, and slopes from 1.0% to 15.0%. Engineers should use caution when extrapolating and using rock sizes and slopes outside of this range.

Equation 13 and 14 are estimations of average interstitial velocity and discharge. Local velocities can vary widely in interstitial flow, and values found using Equation 13 are only a representation of the mean velocity. Similarly, discharges among a rock layer may vary, and Equation 14 estimates the mean discharge across a one square foot area of rock. Design values obtained using Equations 13 and 14 should be applied accordingly.

Application of Equations 13 and 14 should be limited to open channel flow conditions. In both the current study and Abt et al. (1987, 1988) study experimental programs, data were taken in open channel flow conditions, and therefore the data should not be used to predict pressurized interstitial flow behavior. Design engineers should not use the Equations 13 and 14 for closed-

conduit flow. In the case of the all-rock culvert, design engineers should note the limitation mentioned and design the rock size, cross sectional area, and slope (if possible) for a culvert to be flowing just full and with no boundary pressurization.

Recommendations of Use

There is inherent error incurred in the estimation of average interstitial velocity and discharge using Equation 13 and 14. A design allowance of plus or minus 10% is recommended for use when applying Equations 13 and 14. The purpose of providing a design allowance is to allow the engineer discretion and confidence in estimating velocity or discharge. An engineer may need to choose a high, low, or central value in the design allowance given the needs of a project.

A 10% allowance is based off the regression analyses in Chapter 5. Referring to Table 5-2 and Table 5-5, the mean error in percent in the multi-variate nonlinear regression analysis for Equation 13 and Equation 14 is 10.24% and 10.21%, respectively. Figure 6-1 and Figure 6-2 illustrate that most measured versus estimated data points used in the regression for both Equation 13 and Equation 14 fall within the high and low 10% lines.

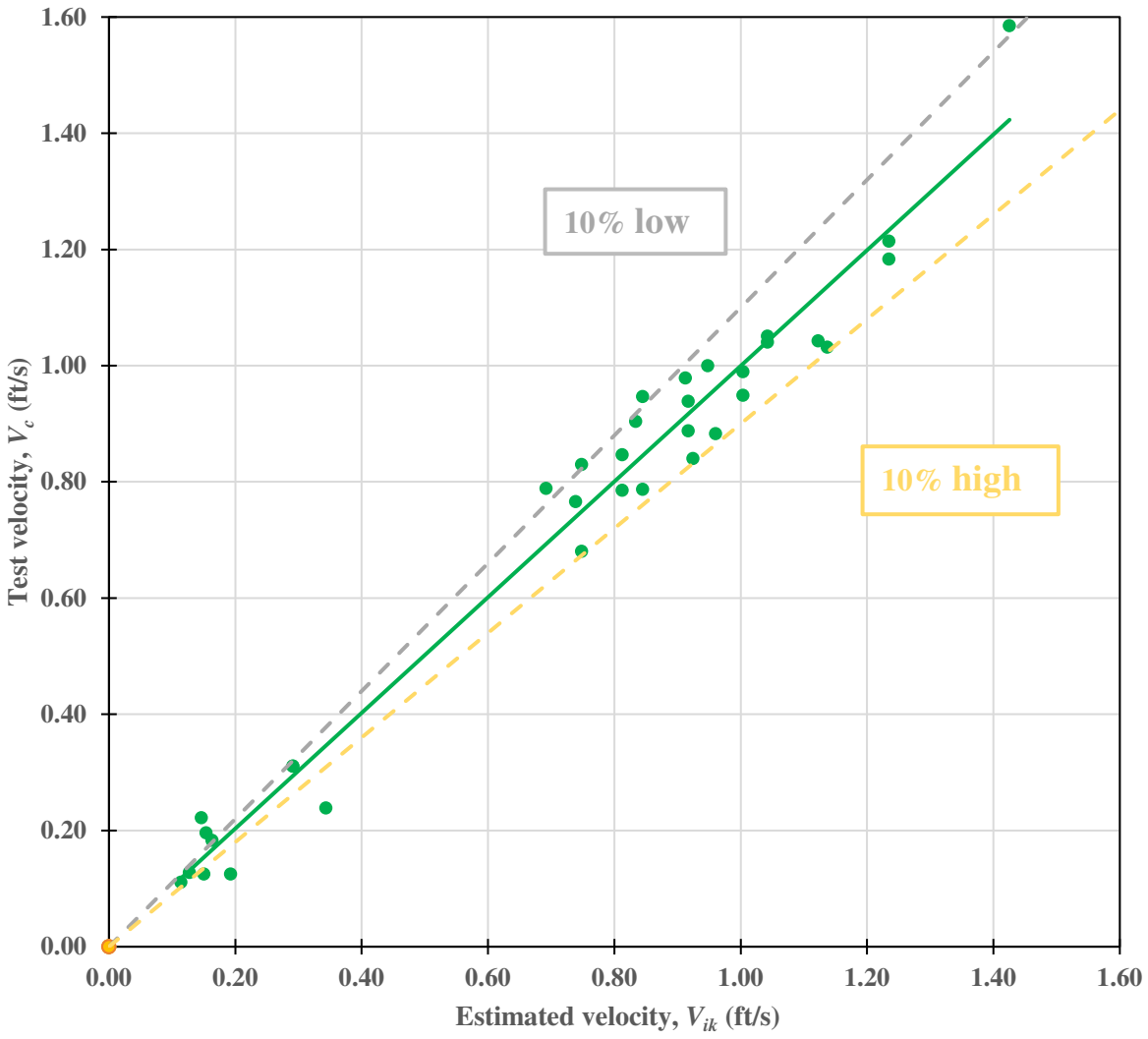

Figure 6-1 Measured versus Equation 13 estimating velocities with margin of error lines at 10%

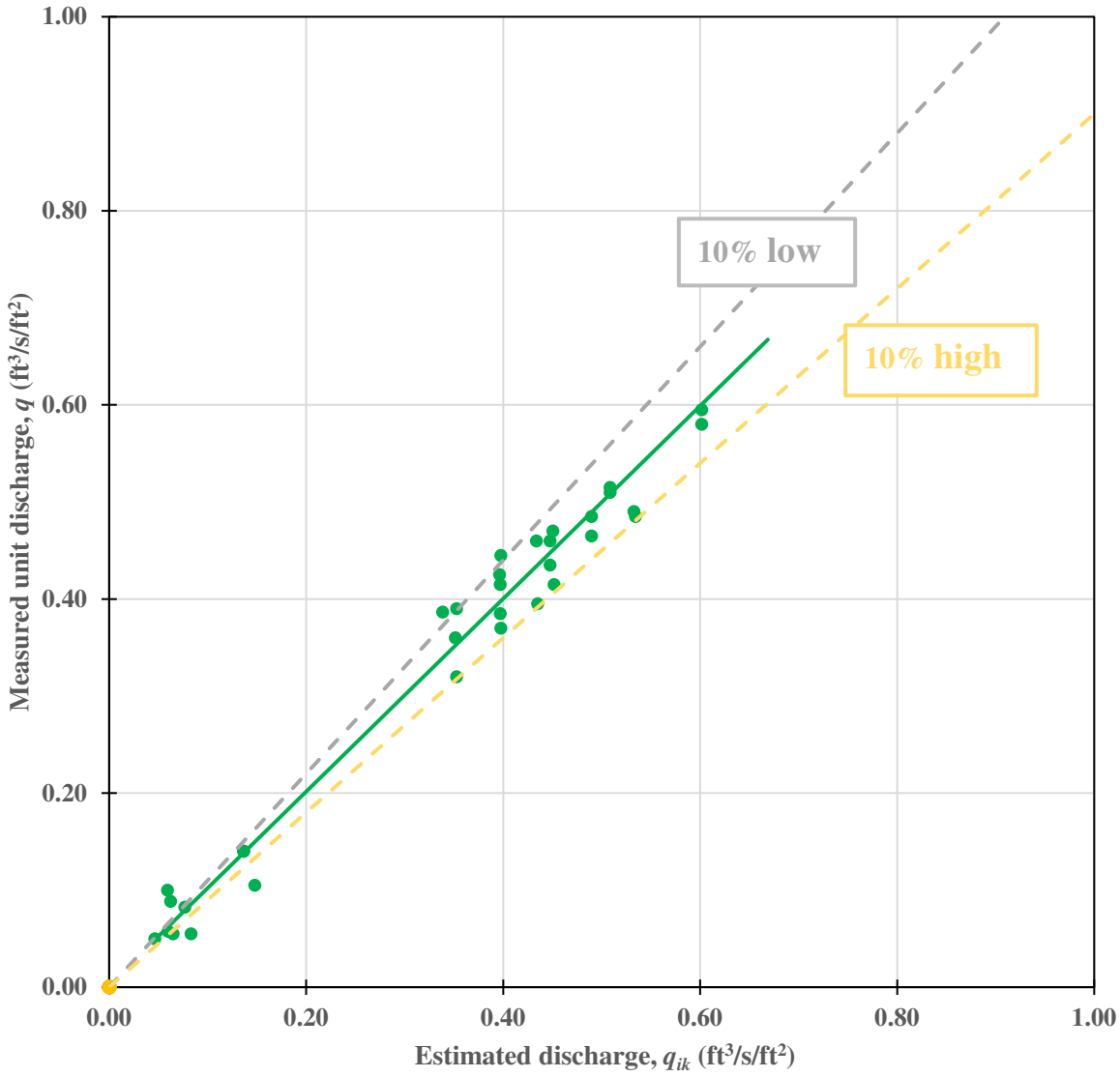

Figure 6-2 Measured versus Equation 14 estimating discharges with margin of error lines at 10%

Conclusions and Future Work

Objectives listed in Chapter 1 are achieved. Design equations to estimate average interstitial velocity and average interstitial discharge were developed by means of analysis and data from a past study (Abt et al. 1987, 1988), data from physical experiments using gabion mattresses, an analysis on the influence of experimental parameters, and a multi-variate nonlinear regression. Design equations (Equation 13 and Equation 14) are recommended for use in engineering design applications including, but not limited to, riprap, gabions, and rockfill fords.

Further studies should improve the range of applicability of the equations presented in this paper. Adding data points that are compatible with the currents sets of data would strengthen the correlations presented in the regression analyses. Separate paragraph? Additionally, data points that have rock sizes and gradations that differ from the current data set would strengthen the range of applicability of resultant regressed equations.

Widening the range of slopes tested may reveal a new trend (leveling out) to velocity and flow rate. There is reason to believe that at a certain point, velocities and discharge may not have a linear correlation with bed slope and hydraulic gradient. A critical flow threshold is hypothesized as flow can only travel so fast through the pores of aggregate rock.

REFERENCES

Abt, S. R., Khattak, M.S., Nelson, J.D., Ruff, J.F., Shaikh, A., Wittler, R.J., Lee, D.W., Hinkle, N.E. (1987). *Development of Riprap Design Criteria by Riprap Testing in Flumes: Phase I*. Colorado State University, Fort Collins, CO, and Oak Ridge National Laboratory, Oak Ridge, TN.

Abt, S. R., Wittler, R.J., Ruff, J.F., LaGrone, D.L., Khattak, M.S., Nelson, J.D., Hinkle, N.E., Lee, D.W. (1988). Development of Riprap Design Criteria by Riprap Testing in Flumes: Phase II. Colorado State University, Fort Collins, CO, and Oak Ridge National Laboratory, Oak Ridge, TN.

Ahmed, N., and Sunada, D. K. (1969). "Nonlinear flow in porous media." *Journal of Hydraulic Engineering*, ASCE, 95(6), 1847.

Bear, Jacob. (1972). *Dynamics of Fluids in Porous Media*. American Elsevier Publishing Company.

Chin, David A. (2013). *Water Resources Engineering*. Chapter 14, Pages 656-76. Pearson Education, Inc. Upper Saddle River, New Jersey.

Federal Highway Administration. (1989). *HEC 11-Design of Riprap Revetment*. Washington, D.C: United States Department of Transportation.

Global Synthetics. (2019). "Link Gabions and Mattresses Design Booklet." ‹https://globalsynthetics.com.au/wp-content/uploads/2016/01/Link-Gabion-Design-Manual.pdf› (July 15, 2019).

Judge, Aaron. (2013). "Measurement of the Hydraulic Conductivity of Gravels Using a Laboratory Permeameter and Silty Sands Using Field Testing with Observation Wells."

Open Access Dissertations. 746. https://scholarworks.umass.edu/open_access_dissertations/746

Julien, Pierre. (2018). *River Mechanics*. Second Edition. Chapter 8, Hillslope and Revetment Stability. Cambridge University Press. New York, NY.

Stephenson, David. (1979). "Rockfill in Hydraulic Engineering." Chapter 2 Flow through rockfill. *Developments in Geotechnical Engineering, Volume 27.* Elsevier Scientific Publishing Company. Amsterdam, The Netherlands

United States Army Corps of Engineers. (1994). "Hydraulic Design of Flood Control Channels." *Engineer Manual 1110-2-1601*. Washington, D.C: Department of the Army.

United States Bureau of Reclamation. (2014). *Embankment Dams-Design Standards No. 13*. Chapter 7-Riprap Slope Protection.

United States Bureau of Reclamation. (1958). "Hydraulic Design of Stilling Basins and Energy Dissipators." *Engineering Monograph No. 25*. Denver, CO.

United States Forest Service. (2006). "Low-Water Crossings: Geomorphic, Biological, and Engineering Design Considerations." United States Department of Agriculture.

Vankataraman, P., Rama Mohan Rao, P. (1998). "Darcian, transitional, and turbulant flow through porous media." *J. Hydr. Div*., ASCE, 124(8).

Ward, J. C. (1964). "Turbulent flow in porous media." *J. Hydr. Div.*, ASCE, 90(5), 1.

APPENDIX A

Equation development for predicting average interstitial velocity and discharge involves testing different equation structures. Equation parameters (D_{50}, D_{10}, C_u, S_o, and g) are arranged in different forms, and a nonlinear power regression is performed. Regression statistics on each form is presented here. Results from the equation chosen for this study are presented in Chapter 5 are omitted from Appendix A. Equation forms are listed:

$$V = a\sqrt{g}D_{50}^{b}D_{10}^{c}C_u^{d}S_o^{f} \tag{15}$$

$$q = l\sqrt{g}D_{50}^{m}D_{10}^{n}C_u^{o}S_o^{p} \tag{16}$$

$$V = a\left(g\sqrt{D_{50}D_{10}}\right)C_u^{b}S_o^{c} \tag{17}$$

$$q = l\left(g\sqrt{D_{50}D_{10}}\right)C_u^{m}S_o^{n} \tag{18}$$

$$V = a(gD_{50}D_{10})^{b}C_u^{c}S_o^{d} \tag{19}$$

$$q = l(gD_{50}D_{10})^{m}C_u^{n}S_o^{o} \tag{20}$$

$$V = D_{50}^{a}D_{10}^{b}C_u^{c}S_o^{d} \tag{21}$$

$$q = D_{50}^{l}D_{10}^{m}C_u^{n}S_o^{o} \tag{22}$$

Regression Results: Equation 15

$$V = a\sqrt{g}D_{50}^{b}D_{10}^{c}C_{u}^{d}S_{o}^{f} \quad (15)$$

Table A-1 Regression statistics for Equation 15

Statistic	Full
Observations	34
DF	29
R^2	0.902
Best Fit Line Slope	1.010
Mean Error (ft/s)	0.092
Mean error (%)	20.500
Iterations	10

Table A-2 Coefficients calculated in regression of Equation 15

Parameters	Value	Standard error
a	1.510	0.422
b	-0.547	1.348
c	1.575	1.199
d	1.202	0.885
f	0.338	0.046

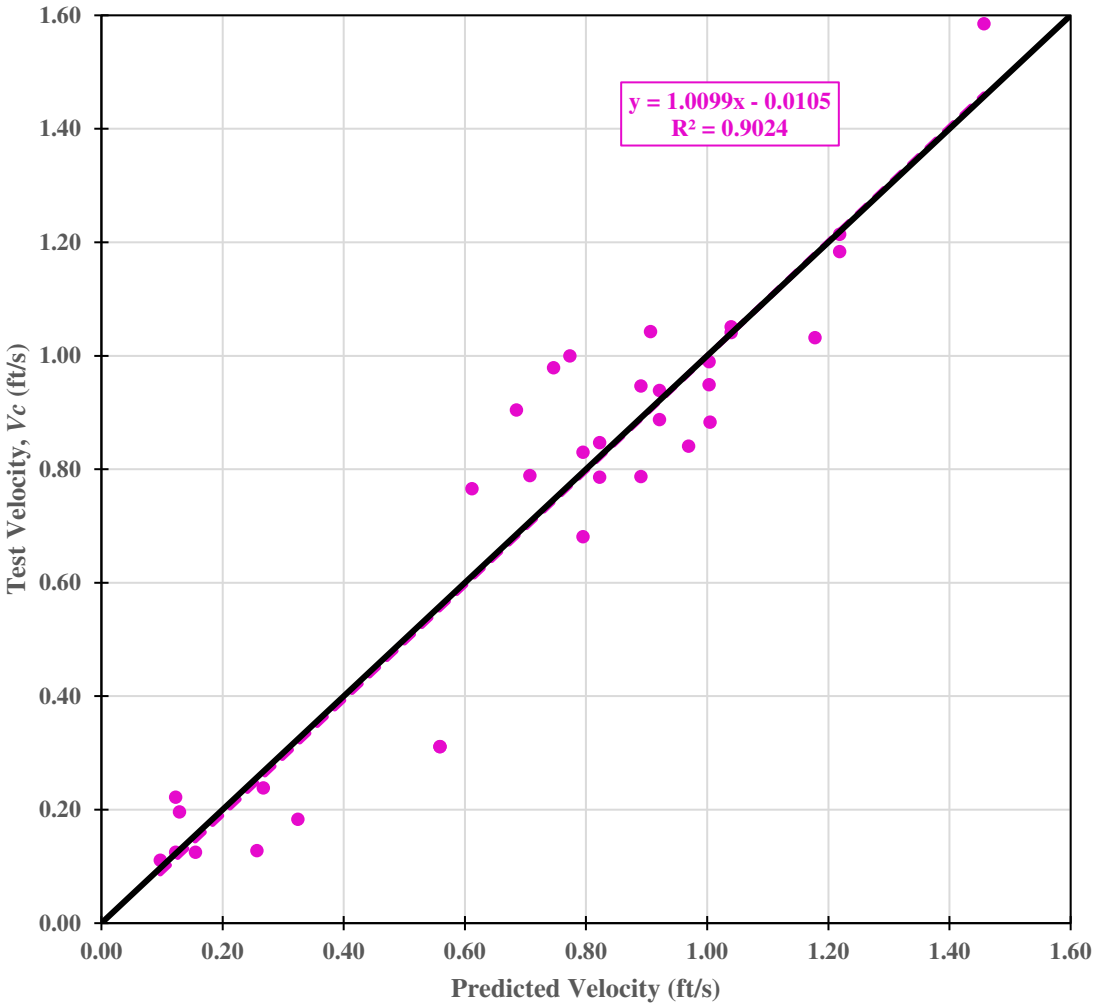

Figure A-1 Measured versus predicted velocity, using Equation 15

Regression Results: Equation 16

$$q = l\sqrt{g}D_{50}^{m}D_{10}^{n}C_{u}^{o}S_{o}^{p} \quad (16)$$

Table A-3 Regression statistics for Equation 16

Statistic	Value
Observations	34
DF	29
R^2	0.946
Best Fit Line Slope	1.067
Mean Error ($ft^3/s/ft^2$)	0.092
Mean error (%)	16.830
Iterations	10

Table A-4 Coefficients calculated in regression of Equation 16

Parameters	Value	Standard error
l	0.585	0.194
m	-2.759	1.187
n	3.652	1.052
o	2.827	0.777
p	0.343	0.042

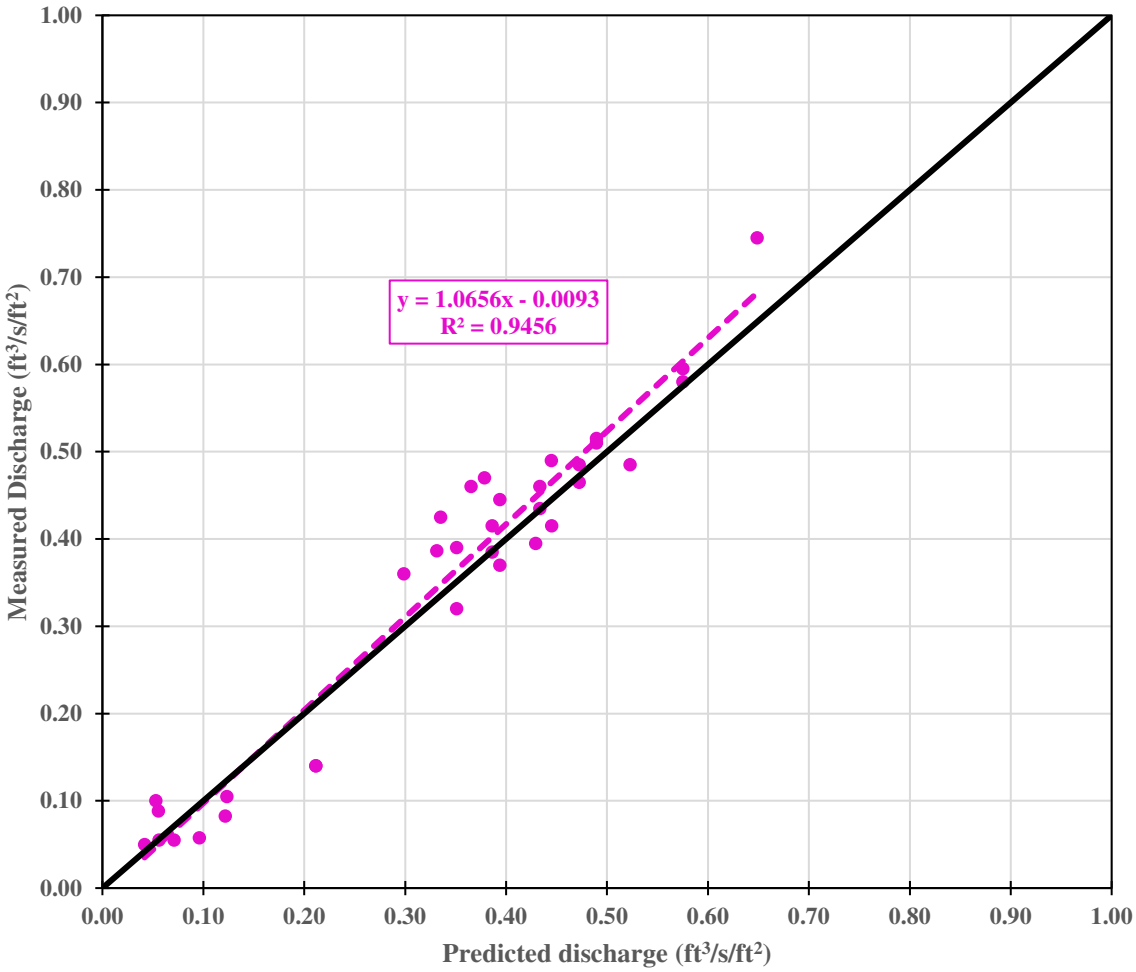

Figure A-2 Measured versus predicted discharge per square foot of rock, using Equation 16

Regression Results: Equation 17

$$V = a\left(g\sqrt{D_{50}D_{10}}\right)C_u^b S_o^c \quad (17)$$

Table A-5 Regression statistics for Equation 17

Statistic	Full
Observations	34
Degrees of Freedom	31
R^2	0.872
Best fit line slope	1.047
Mean error (ft/s)	0.104
Mean error (%)	24.61
Iterations	10

Table A-6 Coefficients calculated in regression of Equation 17

Parameters	Value	Standard error
a	0.248	0.041
b	0.333	0.138
c	0.320	0.055

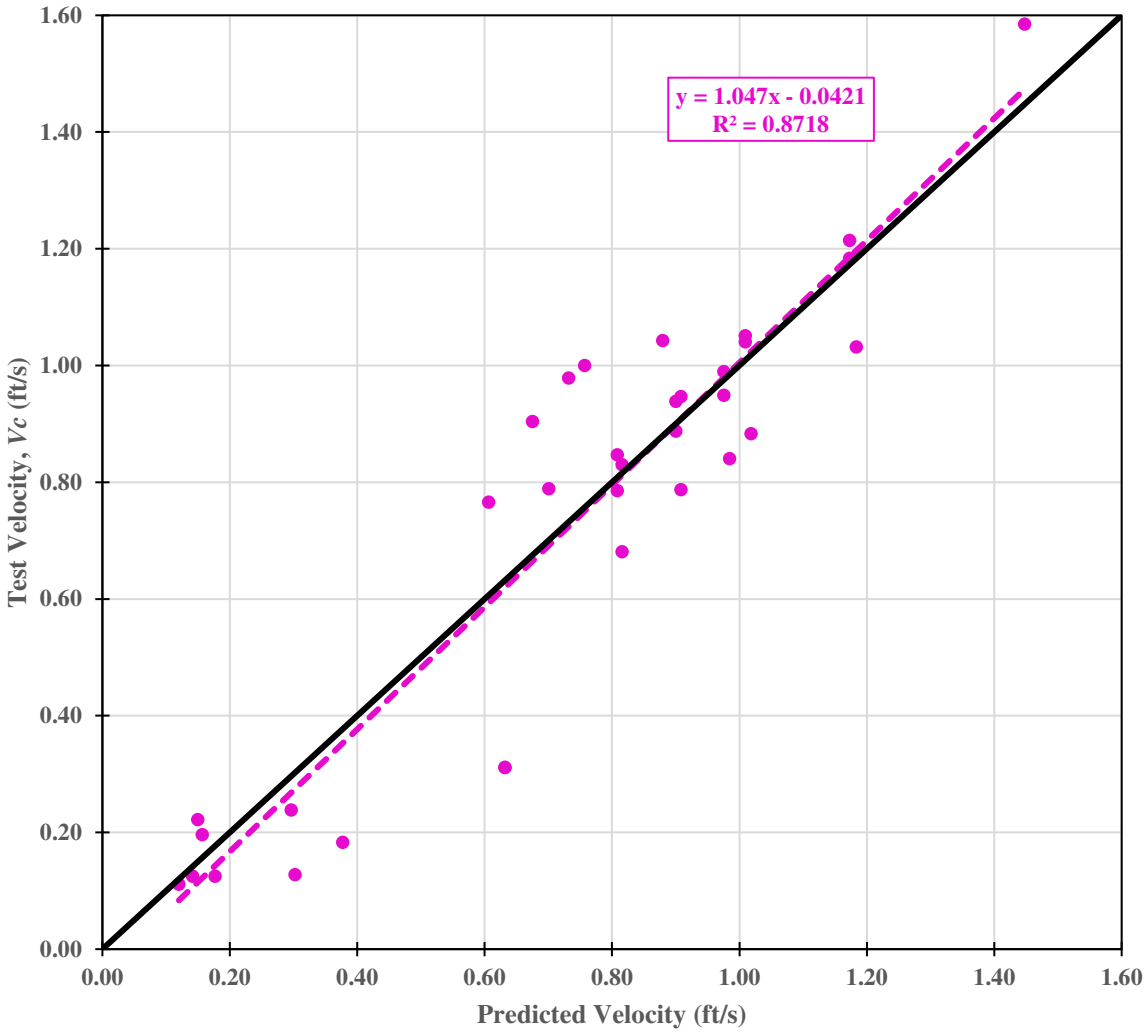

Figure A-3 Measured versus predicted velocity, using Equation 17

Regression Results: Equation 18

$$q = l\left(g\sqrt{D_{50}D_{10}}\right)C_u^m S_o^n \quad (18)$$

Table A-7 Regression statistics for Equation 18

Statistic	Value
Observations	34
Degrees of Freedom	31
R^2	0.873
Best fit line slope	0.812
Mean error ($ft3/s/ft^2$)	0.052
Mean error (%)	27.880
Iterations	10

Table A-8 Coefficients calculated in regression of Equation 18

Parameters	Value	Standard error
l	0.115	0.019
m	0.368	0.142
n	0.313	0.056

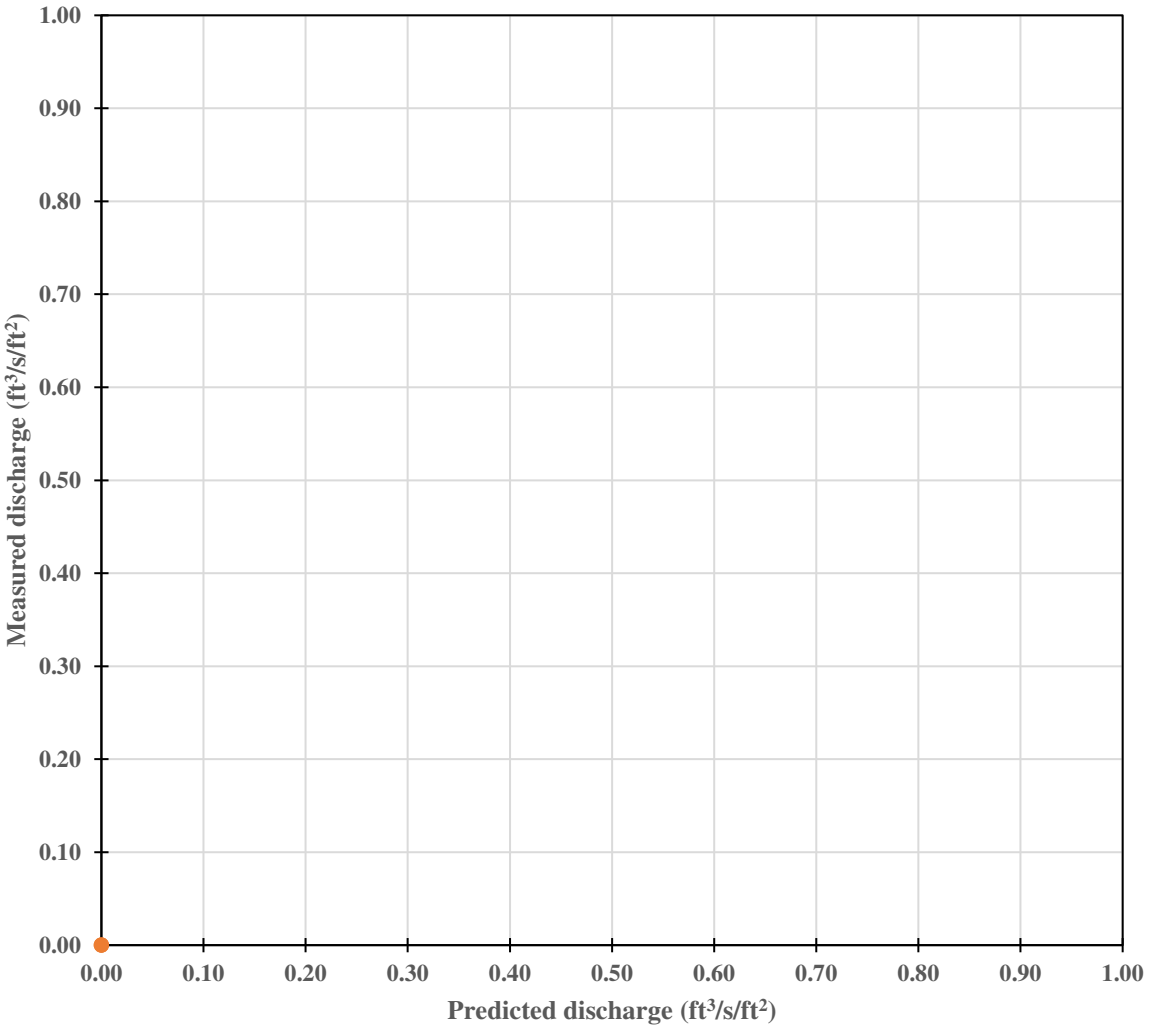

Figure A-4 Measured versus predicted discharge per square foot of rock, using Equation 18

Regression Results: Equation 19

$$V = a(gD_{50}D_{10})^b C_u^c S_o^d \quad (19)$$

Table A-9 Regression statistics for Equation 19

Statistic	Value
Observations	34
Degrees of Freedom	30
R^2	0.876
Best fit line slope	0.986
Mean error (ft/s)	0.101
Mean error (%)	23.071
Iterations	7

Table A-10 Coefficients calculated in regression of Equation 19

Parameters	Value	Standard error
a	1.253	0.241
b	0.605	0.090
c	0.515	0.201
d	0.331	0.055

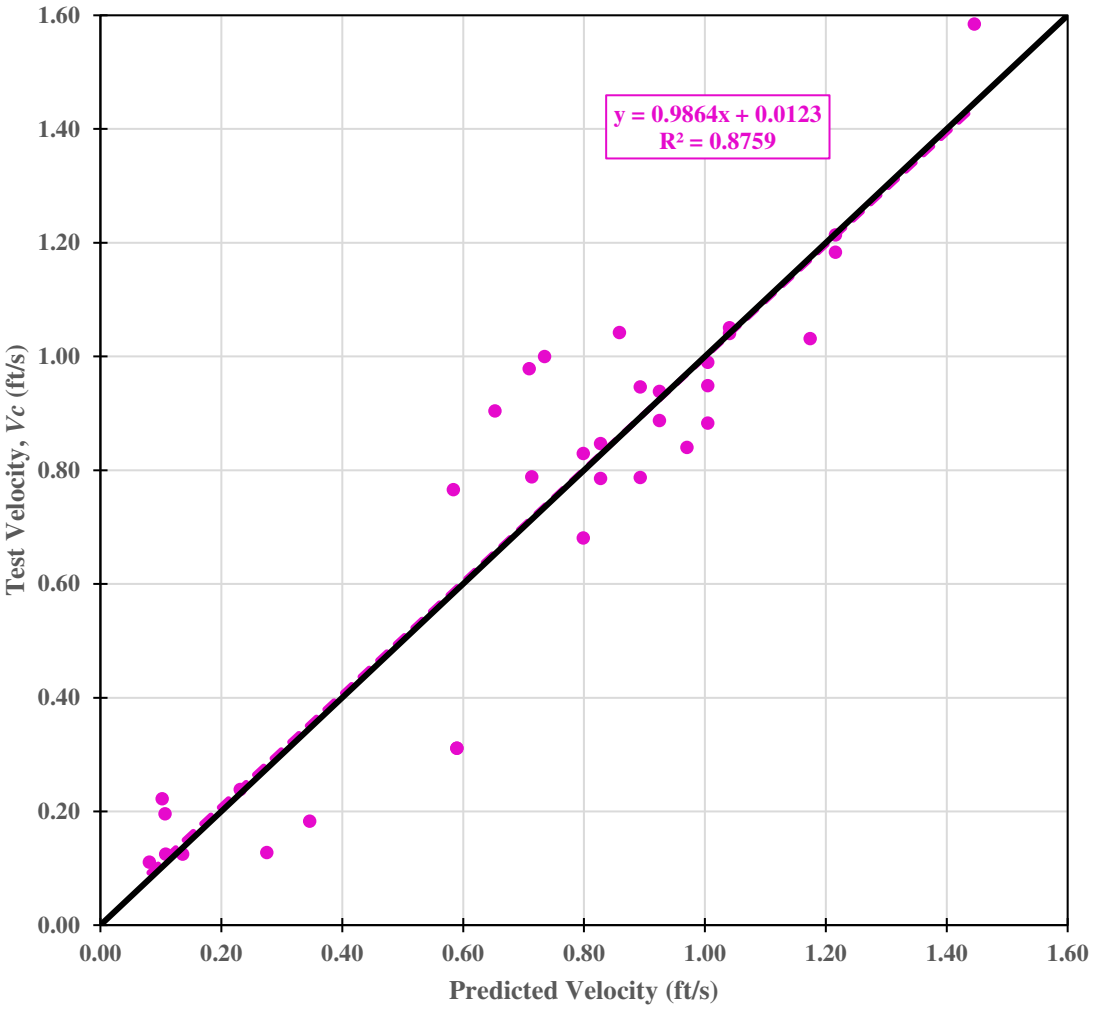

Figure A-5 Measured versus predicted velocity, using Equation 19

Regression Results: Equation 20

$$q = l(gD_{50}D_{10})^m C_u^n S_o^o \quad (20)$$

Table A-11 Regression statistics for Equation 20

Statistic	Value
Observations	34
Degrees of Freedom	30
R^2	0.883
Best fit line slope	0.981
Mean error ($ft^3/s/ft^2$)	0.048
Mean error (%)	24.648
Iterations	8

Table A-12 Coefficients calculated in regression of Equation 20

Parameters	Value	Standard error
l	0.540	0.106
m	0.670	0.095
n	0.662	0.202
o	0.330	0.055

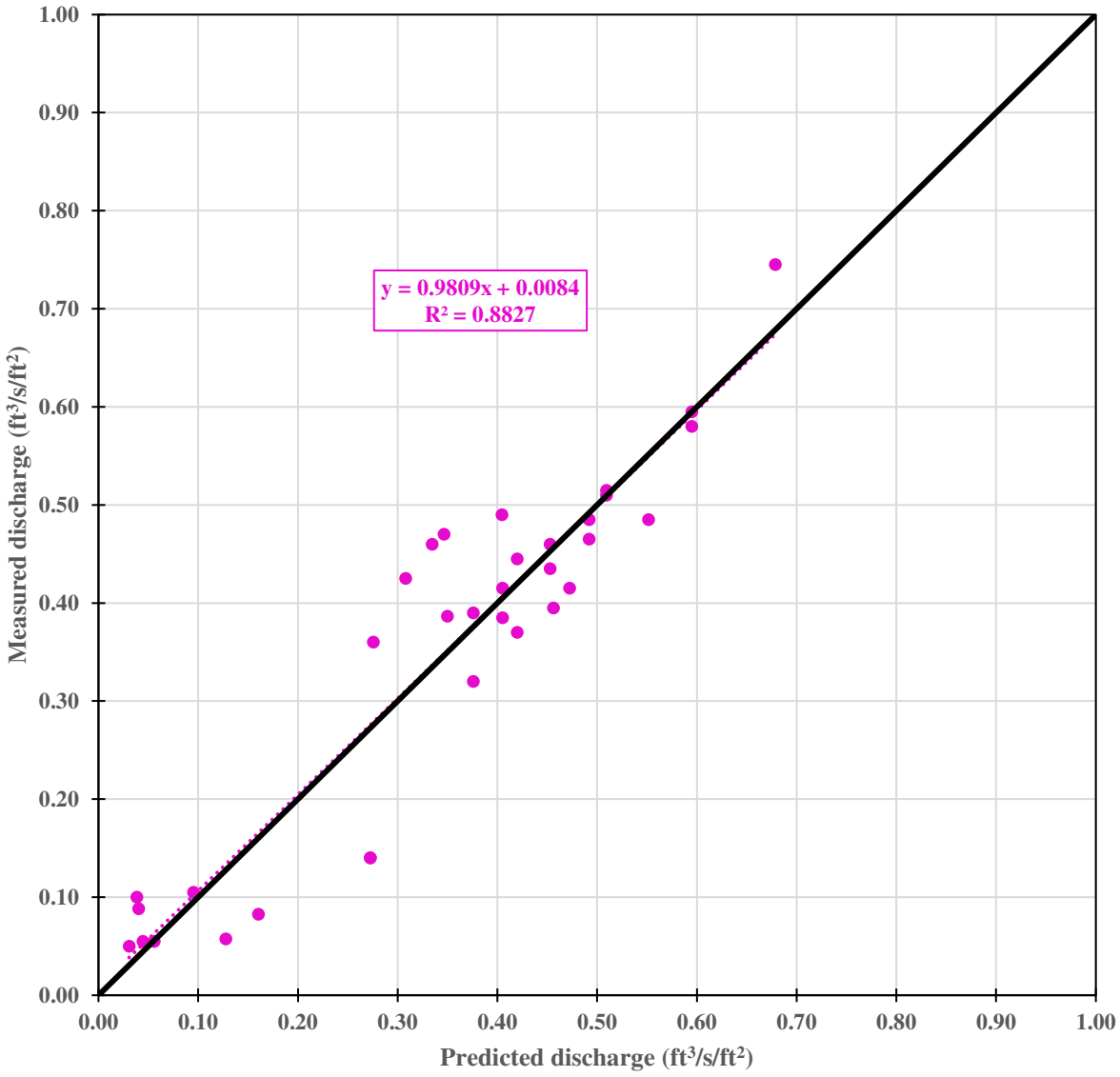

Figure A-6 Measured versus predicted discharge per square foot of rock, using Equation 20

Regression Results: Equation 21

$$V = D_{50}^{a} D_{10}^{b} C_u^{c} S_o^{d} \tag{21}$$

Table A-13 Regression statistics for Equation 21

Statistic	Value
Observations	34
Degrees of Freedom	30
R^2	0.001
Best fit line slope	0.064
Mean error (ft/s)	0.425
Mean error (%)	88.431
Iterations	10

Table A-14 Coefficients calculated in regression of Equation 21

Parameters	Value	Standard error
a	0.144	5.181
b	0.418	5.025
c	2.292	5.082
d	0.202	0.242

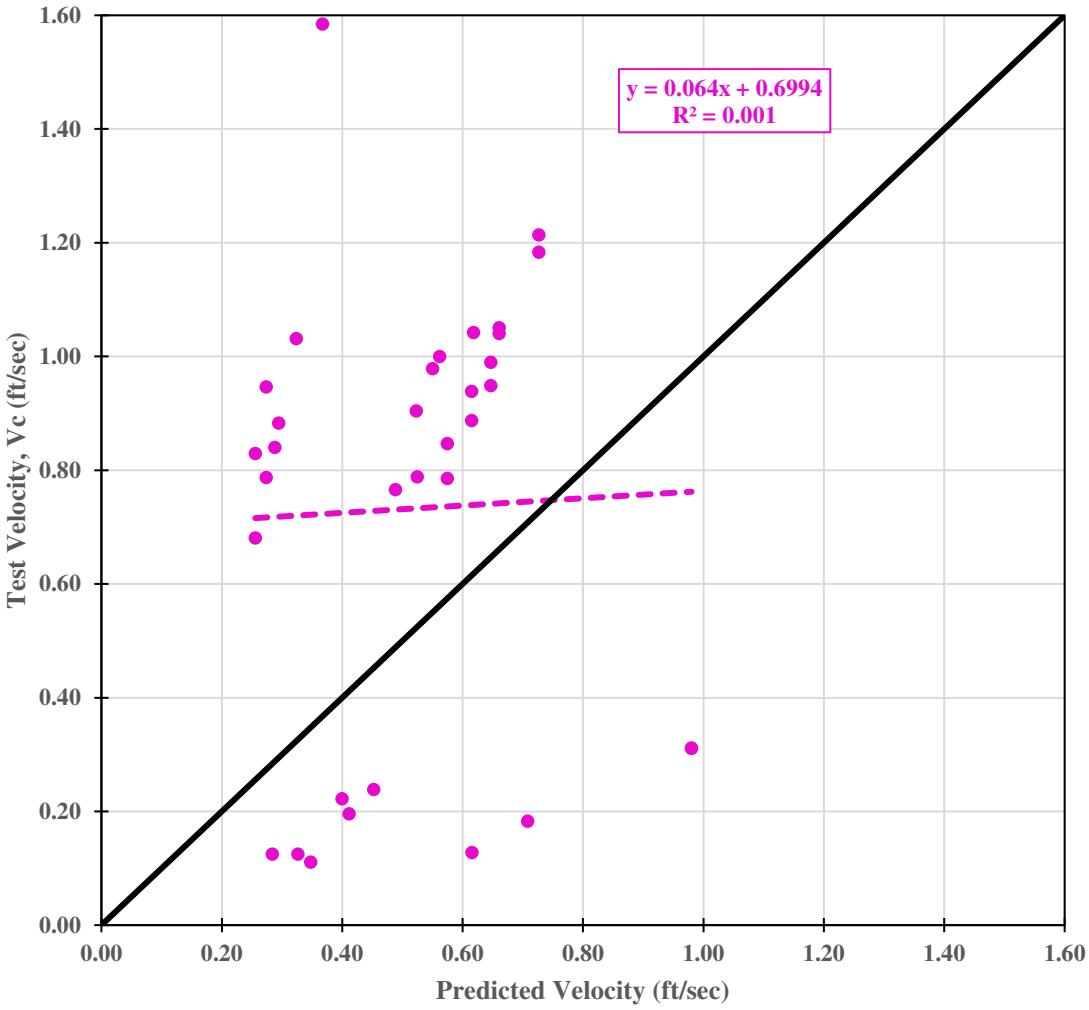

Figure A-7 Measured versus predicted velocity, using Equation 21

Regression Results: Equation 22

$$q = D_{50}^{l} D_{10}^{m} C_u^{n} S_o^{o} \quad (22)$$

Table A-15 Regression statistics for Equation 22

Statistic	Value
Observations	34
Degrees of Freedom	30
R^2	0.927
Best fit line slope	1.293
Mean error ($ft^3/s/ft^2$)	0.049
Mean error (%)	31.362
Iterations	10

Table A-16 Coefficients calculated in regression of Equation 22

Parameters	Value	Standard error
l	-4.147	1.154
m	4.507	1.084
n	3.301	0.837
o	0.137	0.043

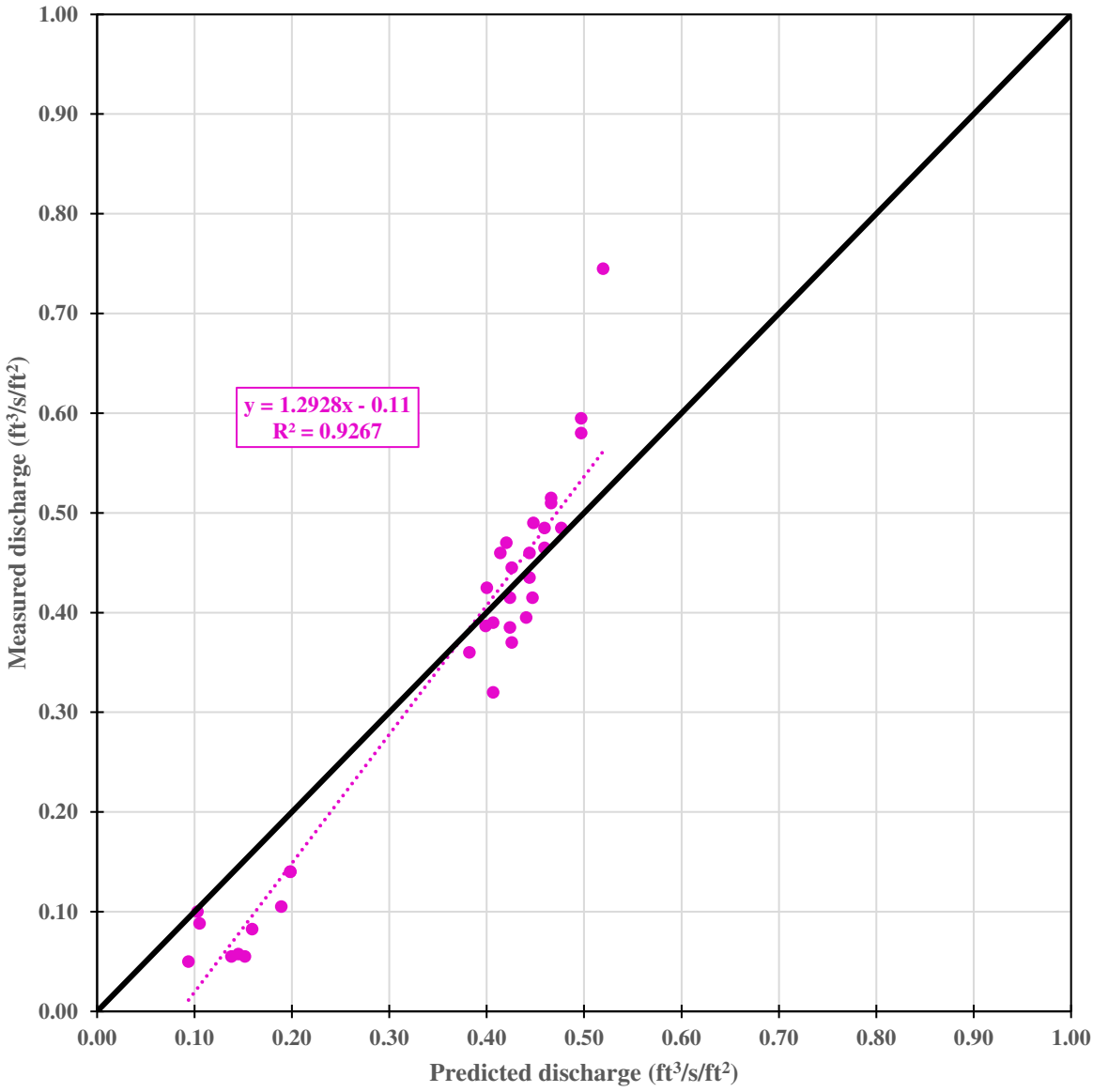

Figure A-8 Measured versus predicted discharge per square foot of rock, using Equation 22